

As easy as PIE: understanding when pruning causes language models to disagree

Anonymous ACL submission

Abstract

Language Model (LM) pruning compresses the model by removing weights, nodes, or other parts of its architecture. Typically, pruning focuses on the resulting efficiency gains at the cost of effectiveness. However, when looking at how individual data points are affected by pruning, it turns out that a particular subset of data points always bears most of the brunt (in terms of reduced accuracy) when pruning, but this effect goes unnoticed when reporting the mean accuracy of all data points. These data points are called PIEs and have been studied in image processing, but not in NLP. In a study of various NLP datasets, pruning methods, and levels of compression, we find that PIEs impact inference quality considerably, regardless of class frequency, and that BERT is more prone to this than BiLSTM. We also find that PIEs contain a high amount of data points that have the largest influence on how well the model generalises to unseen data. This means that when pruning, with seemingly moderate loss to accuracy across all data points, we in fact hurt tremendously those data points that matter the most. We trace what makes PIEs both hard and impactful to inference to their overall longer and more semantically complex text. These findings are novel and contribute to understanding how LMs are affected by pruning.

1 Introduction

Deep neural networks (NNs) are becoming increasingly larger, with remarkable improvements to their inference capabilities, but also very high computational demands. The latter has motivated research in the area of NN pruning, whose goal is to reduce a model (in terms of its parameters, nodes, layers, or any other aspect of its architecture) to a smaller version, without significant loss of inference quality. Pruning has been shown to produce smaller, hence more efficient NNs, with small loss to their effectiveness (Li et al., 2020a; Hooker

Class: neutral
Premise: A group of seven individuals wearing rafting gear, white water raft down a river.
Hypothesis: Seven men and women are in a yellow boat.
Unpruned model prediction: entailment
Pruned model prediction: neutral
Class: entailment
Premise: A woman is painting a mural of a woman’s face.
Hypothesis: There is a woman painting.
Unpruned model prediction: entailment
Pruned model prediction: contradiction

Table 1: Examples where pruned and unpruned models disagree (from the SNLI dataset).

et al., 2019). Similar findings are also reported when pruning Language Models (LMs) (Gupta and Agrawal, 2022; Wang et al., 2020; Sun et al., 2023; Sanh et al., 2020a; Michel et al., 2019) in NLP.

When pruning NNs, typically the focus is on the high efficiency gains achieved at the cost of effectiveness, commonly measured in terms of test set accuracy. However, when zooming in on precisely how individual data points are affected by pruning, it turns out that models of similar accuracy scores can have notably different weights and therefore make wildly different inferences on a subset of data points. In other words, the similar accuracy scores between pruned and unpruned models do not mean that pruning affects all data points in a uniform way, but rather that some parts of the data distribution are much more sensitive to pruning than others. This effect can go unnoticed when one measures pruning effectiveness in terms of mean accuracy, because taking the mean can hide such important score variations in the data. However, this does not change the fact that certain types of data are dispro-

064 portionately impacted by pruning, which begs the
065 question: what are the characteristics of these data
066 points and how important is their detection?

067 In response to this, *Pruned Identified Exemplars*
068 (PIEs) are defined as the subset of data points where
069 pruned and unpruned models disagree (Hooker
070 et al., 2019) (see example in Table 1). Studies
071 in image processing reveal that PIEs are harder to
072 classify, not only for NNs, but also for humans,
073 because they a) tend to be mislabeled (ground truth
074 noise), b) may have overall lower quality (inherently
075 noisy signal), or c) may depict multiple objects
076 (more challenging task) (Hooker et al., 2019).
077 Hence, this subset of data points where pruned and
078 unpruned models tend to disagree are also some of
079 the most difficult data points for the model to handle.
080 PIEs are those critical data points on which we
081 would suffer the most damage, if the model were
082 to be deployed out in the wild. Despite this, to our
083 knowledge, PIEs have not been studied in NLP.

084 Motivated by this gap in understanding how LMs
085 are actually affected by pruning, we study whether
086 PIEs exist in text, what are their textual character-
087 istics, and what this practically means for inference.
088 Using eight pruning methods on two different
089 LM architectures (BiLSTM and BERT) and four
090 common NLP datasets for sentiment classification,
091 document categorisation and natural language infer-
092 ence, we contribute the first study of PIEs in LM
093 pruning for NLP. Our empirical analysis shows that
094 there is always a subset of data points where pruned
095 and unpruned models disagree, and that this sub-
096 set is larger for BERT than BiLSTM. We also find
097 that these data points, namely PIEs, are overall se-
098 mantically more complex, contain on average more
099 difficult words, and have generally longer text than
100 the rest of the data. Furthermore, we find that PIEs
101 contain a high amount of *influential examples*, i.e.
102 data points that have the largest influence on how
103 well the model generalises to unseen data. These
104 findings are novel, and practically, they mean that,
105 when pruning LMs for efficiency, and in particu-
106 lar BERT, with seemingly small drops to overall
107 accuracy, we are in fact impacting notably the ac-
108 curacy of a particular subset of our data, which
109 also happens to be the most critical part of our data
110 with respect to how well the model is expected to
111 generalise to unseen data, or more simply put, how
112 well the model actually learns. This effect is much
113 more pronounced for BERT than for BiLSTM.

2 Pruned Identified Exemplars (PIEs) 114

We formally define PIEs and propose an extension
of this definition to multi-label classification. 115 116

2.1 Formal definition of PIEs 117

Pruned Identified Exemplars (PIEs) are data in-
stances¹ where the predictions of pruned and un-
pruned models differ (Hooker et al., 2019). As-
sume a single-label classification task, where each
instance x belongs to a single class. Let $P =$
 $\{p_1, \dots, p_N\}$ be the set of N different initializa-
tions of the pruned model, and $U = \{u_1, \dots, u_N\}$
the set of N different initializations of the unpruned
model.² Let $m(P, x)$ be the majority class assigned
to x over all the initializations of the pruned model
after training. This is computed as the most fre-
quently predicted class for the instance x across all
 N initializations in P , i.e., the mode of the N pre-
dicted classes.³ Similarly, $m(U, x)$ is the most fre-
quent class predicted by the unpruned model initial-
izations. Then, x is a PIE if $m(P, x) \neq m(U, x)$,
i.e., the majority class assigned to x by the pruned
and unpruned model is different. 118 119 120 121 122 123 124 125 126 127 128 129 130 131 132 133 134 135

2.2 PIEs in multi-label classification 136

We extend the above definition of PIEs to multi-
label classification, where an instance x can belong
to more than one class. We treat multi-label classi-
fication as multiple single-label classifications: an in-
stance x is a PIE, if there exists a class such that the
pruned and unpruned models disagree. Let $\tilde{m}(P, x)$
be the set of majority classes assigned to x over all
the initializations of the pruned models. A class
is assigned to the set of majority classes if $> N/2$
initializations of the pruned model predict that x be-
longs to that class. Similarly, $\tilde{m}(U, x)$ is the set of
majority classes assigned by the unpruned model.
Then, x is a PIE if $\tilde{m}(P, x) \neq \tilde{m}(U, x)$, i.e., the
sets of majority classes predicted for x by the
pruned and unpruned models differ. The inequality
between $\tilde{m}(P, x) \not\subseteq \tilde{m}(U, x)$ and $\tilde{m}(P, x) \not\supseteq$
 $\tilde{m}(U, x)$ means that x is a PIE even if the pruned
and unpruned model disagree only on a single class. 137 138 139 140 141 142 143 144 145 146 147 148 149 150 151 152 153 154

Holste et al. (2023) propose the following al-
ternative way of selecting PIEs in a multi-label
setting. For each instance, they compute the av-
erage prediction over all initializations. Then, the 155 156 157 158

¹We will use the terms *instance* and *data point* interchangeably henceforth.

² N must be the same for pruned and unpruned models.

³In case of ties, classes are sorted ascendingly by their associated number, and the first class is assigned.

Dataset	# train	# test	# val	# classes	Classification
IMDB	20000	25000	5000	2	single-label
SNLI	549367	9824	9842	3	single-label
Reuters	6737	1429	1440	23	multi-label
AAPD	53840	1000	1000	54	multi-label

Table 2: Dataset statistics after preprocessing.

Scoring → Scheduling ↓	Impact Based	Magnitude	Random
Iterative + Weight Rewinding	IIBP-WR	IMP-WR	-
Iterative + Fine tuning	IIBP-FT	IMP-FT	IRP-FT
At Initialization	IBP-AI	MP-AI	RP-AI

Table 3: Our 8 pruning methods. *Random* cannot be combined with *Weight Rewinding* because weights that are rewinded to their initial values are not random.

instances are ranked by the average prediction, and agreement is measured as the Spearman rank correlation between the rankings for the pruned and unpruned models. The 5th percentile of instances with highest disagreement (lowest Spearman rank correlation) are considered PIEs. This approach does not allow to exactly quantify the amount of PIEs for the pruned and unpruned models. In addition, in Holste et al. (2023), an instance can be considered as non PIE even if there is disagreement between the pruned and unpruned models, simply because that instance is outside the 5th percentile. Our definition of PIEs is stricter than Holste et al.’s (2023), since disagreement even on a single class determines the instance to be a PIE.

3 Study design

Our aim is to study whether PIEs exist in text data, what are their textual characteristics, and what this practically means for inference. We present the datasets, LMs, and pruning methods of our study.

Datasets. We use two single-label datasets: IMDB (Maas et al., 2011) for sentiment analysis, and SNLI (Bowman et al., 2015) for natural language inference. We also use two multi-label datasets for document categorisation: Reuters-21578⁴, and AAPD (Yang et al., 2018). Statistics are in Table 2 (see Appendix A.2 for preprocessing details).

Language Model Architectures. We select two common types of LMs to represent both transformers and Recurrent Neural Networks (RNNs): BERT (Devlin et al., 2019), and bidirectional

⁴<https://www.daviddlewis.com/resources/>.

LSTM (BiLSTM) (Hochreiter and Schmidhuber, 1997). We train BiLSTM from scratch, but we finetune a pretrained version of BERT_{BASE}. See Table 5 in Appendix A.1 for details on the LMs, and Appendix A.1 for our tuning methodology.

Pruning methods. We use eight common pruning methods, shown in Table 3. Each of them is a combination of *scheduling* and *scoring*.

Scheduling controls the moment and frequency of the pruning iterations during training. We use two scheduling variations: (i) pruning the model before training (*at initialization*), and (ii) pruning in multiple iterations during training (*iterative*). Only for iterative pruning, we use two tuning strategies: *finetuning* and *weight rewinding*. In finetuning, we retrain the model after pruning and update its weights. In weight rewinding, we rewind weights to their initial state (Frankle and Carbin, 2019).

Scoring refers to selecting which weights to prune. A score is given to each LM weight, and the weights with the lowest score according to a threshold are pruned. We use 3 scoring variations: 1. The score is the absolute value of a weight (*magnitude based pruning* (Frankle and Carbin, 2019)); 2. The score is the weight multiplied by its accumulated gradient on 100 randomly sampled data points of the training set (*impact based pruning* (Lee et al., 2019)); 3. The score is randomly assigned a value between 0 and 1 (*random* (Jin et al., 2022)).

Overall, we prune each LM at 20%, 50%, 70%, 90%, 99% (see Table 5 in Appendix A.1 for details). For each configuration, we train 30 initializations. This results in 9840 runs (= 2 LMs x 4 datasets x 8 pruning methods x 5 pruning thresholds x 30 initializations + 2 LMs x 4 datasets x 30 unpruned model initializations), that require ca. 28000 AMD MI250X GPU hours. Our tuning methodology for pruning is detailed in Appendix A.4.

4 Experimental findings

We show how pruning impacts inference, the role of PIEs, and the textual characteristics of PIEs.

4.1 Pruning and occurrence of PIEs

Figure 1 shows the accuracy/F1 of pruned versus unpruned models (see Table 6 in Appendix A.1 for details on the number of parameters pruned). We see that pruning BERT/BiLSTM up to 50% gives overall tolerable drops to accuracy/F1 for most pruning methods. IIBP-FT is the pruning method with the overall smallest drop in accuracy/F1 com-

pared to the unpruned model, and even outperforms the unpruned BiLSTM at times. We also see that, while unpruned BERT outperforms unpruned BiLSTM, pruning BERT hurts accuracy/F1 more than pruning BiLSTM, especially for pruning at 70%-99%. Hence **BERT is more sensitive to pruning than BiLSTM**, indicating that parameters in BERT are not as easily disposable as in BiLSTM. Otherwise put, BERT seems to make better use of its parameters than BiLSTM, because their removal has a bigger impact on it than on BiLSTM.

Table 4 shows the % of all data points⁵ that are PIEs per model, dataset, pruning method and pruning threshold. We see that, as the pruning threshold increases, so does the proportion of PIEs, with very few marginal exceptions. This means that the particular subset of data points where unpruned and pruned models disagree becomes larger, the more we prune. In Table 4 we shade the PIEs of the best and worst pruned model (according to their accuracy/F1 in Figure 1) as green and gray respectively. We see that the best pruned model (green) has almost always a smaller percentage of PIEs than the worst pruned model (gray), per pruning threshold. In other words, **as the amount of PIEs increases, overall accuracy/F1 lowers, meaning that PIEs clearly impact inference quality**.

For the multi-label datasets, it is important to know, not only the proportion of data points that are PIEs, but also their distribution across classes. So, Figure 2 plots the distribution of all data points versus PIEs, across classes, for IIBP-FT, which is the pruner with the best overall F1 in Figure 1. The plots of the other configurations are in Appendix B.1. We show PIEs resulting from the least (20%) and most (99%) pruning, which should capture the lowest and highest % of PIEs according to Table 4. Figure 2 shows that PIEs are found across all classes of the dataset, from the least frequent to the most frequent class, and roughly follow the distribution of all data points across classes. This observation, combined with the findings of Table 4, means that **the impact of PIEs on inference quality is considerable on all classes of the dataset, regardless of class frequency**.

To probe further into the extent of this impact, Figure 3 shows accuracy only on PIEs versus accuracy on all data points, for BERT and SNLI. The plots of the other configurations are in Appendix

		Single-label						
		Pruner	20%	50%	70%	90%	99%	
IMDB	BERT	IIBP-WR	7	10	10	10	11	
		IIBP-FT	4	10	13	13	11	
		IBP-AI	8	10	10	10	50	
		IMP-WR	4	9	11	12	50	
		IMP-FT	3	10	14	13	50	
		MP-AI	6	10	10	12	50	
	IMDB	IRP-FT	8	13	12	50	50	
		RP-AI	10	10	10	50	50	
		BiLSTM	IIBP-WR	2	3	4	7	10
			IIBP-FT	5	5	5	5	3
			IBP-AI	2	5	7	10	16
			IMP-WR	2	3	4	3	11
	IMP-FT		5	5	5	5	5	
	MP-AI		2	5	6	9	16	
	SNLI	IRP-FT	5	5	5	3	29	
		RP-AI	2	4	6	9	18	
		BERT	IIBP-WR	7	13	16	27	35
			IIBP-FT	3	5	8	13	28
IBP-AI			6	12	18	34	47	
IMP-WR			5	11	16	30	66	
IMP-FT	3		6	12	16	66		
MP-AI	5		12	27	35	66		
SNLI	IRP-FT	4	11	17	66	66		
	RP-AI	8	26	32	66	66		
	BiLSTM	IIBP-WR	4	5	7	16	29	
		IIBP-FT	6	5	5	6	23	
		IBP-AI	4	7	11	23	39	
		IMP-WR	5	5	5	14	62	
IMP-FT		6	6	5	8	32		
MP-AI		4	7	12	20	62		
Reuters	IRP-FT	6	5	5	16	46		
	RP-AI	4	8	13	23	62		
	AAPD	BERT	IIBP-WR	5	8	16	31	100
			IIBP-FT	5	6	7	10	32
			IBP-AI	6	18	35	84	100
			IMP-WR	4	6	14	100	100
IMP-FT			5	6	8	23	100	
MP-AI			5	12	32	100	100	
Reuters		IRP-FT	5	10	24	100	100	
		RP-AI	7	34	41	100	100	
		BiLSTM	IIBP-WR	4	5	7	14	37
			IIBP-FT	4	5	5	5	9
			IBP-AI	4	7	14	34	44
			IMP-WR	5	5	6	7	29
IMP-FT			5	4	4	6	13	
MP-AI			5	6	9	19	33	
AAPD		IRP-FT	5	5	6	7	31	
		RP-AI	4	7	10	22	35	
		BERT	IIBP-WR	31	40	48	59	81
			IIBP-FT	29	37	45	51	63
	IBP-AI		34	48	59	78	100	
	IMP-WR		31	38	49	79	100	
IMP-FT	28		40	45	56	100		
MP-AI	34		47	57	94	100		
AAPD	IRP-FT	33	63	62	100	100		
	RP-AI	38	59	76	100	100		
	BiLSTM	IIBP-WR	26	34	39	64	88	
		IIBP-FT	41	40	37	28	59	
		IBP-AI	22	33	53	82	100	
		IMP-WR	26	32	38	56	83	
IMP-FT		39	41	37	34	69		
MP-AI		21	30	41	62	86		
AAPD	IRP-FT	41	36	30	44	88		
	RP-AI	24	35	49	67	87		

Table 4: Percentage of datapoints that are PIEs per configuration. Green and gray mark the percentages of datapoints that are PIEs for the best (green) and worst (gray) pruner per dataset and pruning threshold.

⁵From now on, whenever we refer to all data points, we mean all data points in the test set, unless otherwise specified.

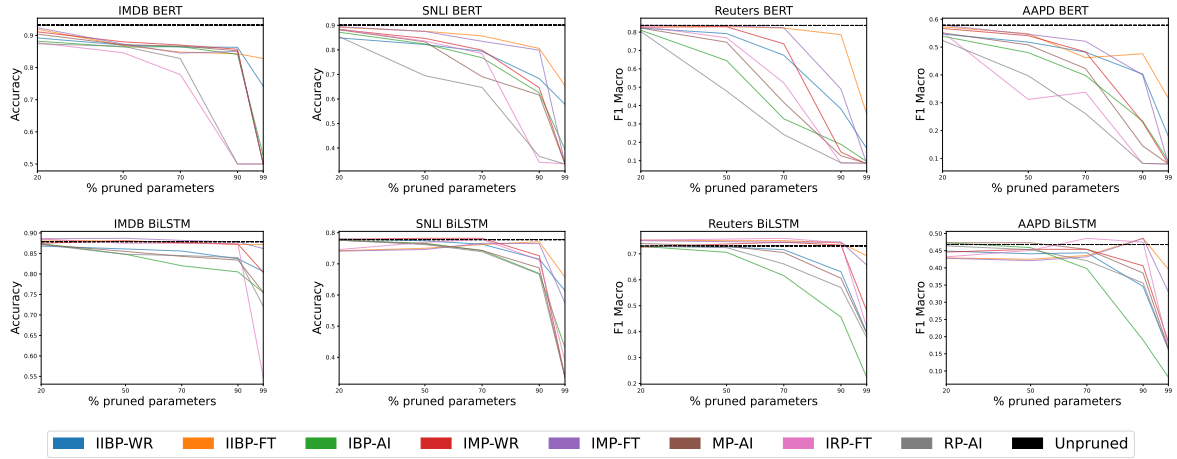


Figure 1: Accuracy/F1 (y axis) of unpruned and pruned LMs per pruning threshold (x axis), over 30 initializations.

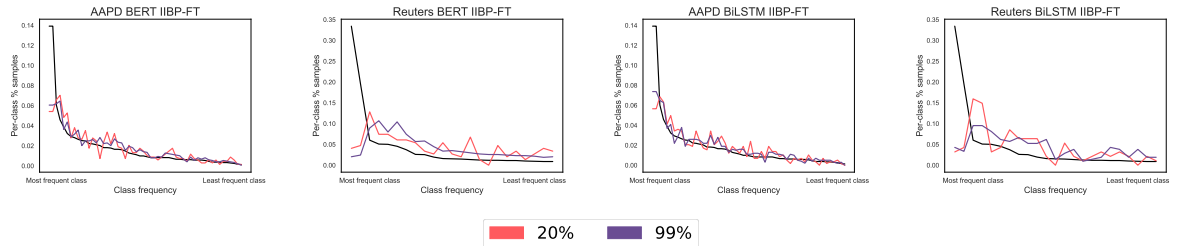


Figure 2: Distribution of all data points and of PIEs at 20% and 99% pruning, across classes sorted by frequency (x axis), for the multi-label datasets (test set) and IIBP-FT pruner.

288 B.1 and have overall similar trends. We see that
 289 accuracy is overall lower on PIEs (orange) than
 290 on all data points (blue), for both pruned and un-
 291 pruned models, with few marginal exceptions for
 292 99% pruning and BiLSTM, where the scores are
 293 almost the same. The fact that accuracy is lower for
 294 PIEs than for all data points confirms the findings
 295 reported above. However, interestingly, Figure 3
 296 also shows that the impact of pruning upon accu-
 297 racy is much larger on the subset of PIEs than on all
 298 data points: the gap between the two orange lines
 299 (PIEs) in Figure 3 is notably larger than the gap
 300 between the two blue lines (all data points). Even
 301 when pruning 20%-50%, which according to Fig-
 302 ure 1 has overall small drops to the mean accuracy
 303 of all data points for most pruning methods, still,
 304 the drop in accuracy to the data points of the dataset
 305 that are PIEs is much larger. This means that **PIEs**
 306 **always bear most of the brunt when pruning,**
 307 **but this effect goes unnoticed when reporting**
 308 **the mean accuracy over all data points.**

309 4.2 Influential examples in PIEs

310 The above findings suggest that PIEs are hard for
 311 inference. Next, we try to quantify this hardness, by

312 studying how many of the PIEs are in fact *influen-*
 313 *tial examples*, i.e. data points that have the largest
 314 influence on how well the model generalises to un-
 315 seen data, irrespective of whether this influence is
 316 positive or negative. We do this using the EL2N
 317 score (Paul et al., 2021) as per Jin et al. (2022).

318 Given a model with weights w_t during training
 319 iteration t , and given an example (x, y) where x
 320 is the input and y is its label, $EL2N(x, y)$ is the
 321 L2 distance between the predicted probabilities
 322 $p(w_t, x)$ during t^6 and the one-hot label:

$$323 EL2N(x, y) = \mathbb{E} [\|p(w_t, x) - y\|_2] \quad (1)$$

324 Examples are grouped into 20 bins based on their
 325 EL2N score percentiles. Higher EL2N scores mean
 326 that the model undergoes larger weight updates
 327 when the example is presented early in training.
 328 So, the bigger the weight changes, the higher the
 329 EL2N score, and the higher the influence of an
 330 example. Note that the above takes place during
 331 training, so we obtain PIEs on the training set.

⁶As the EL2N score is not reliable until at least one epoch of fine-tuning has been computed (Fayyaz et al., 2022), we only monitor the scores after the model has undergone training for at least one epoch (the first epoch that exceeds 30% of the total training epochs).

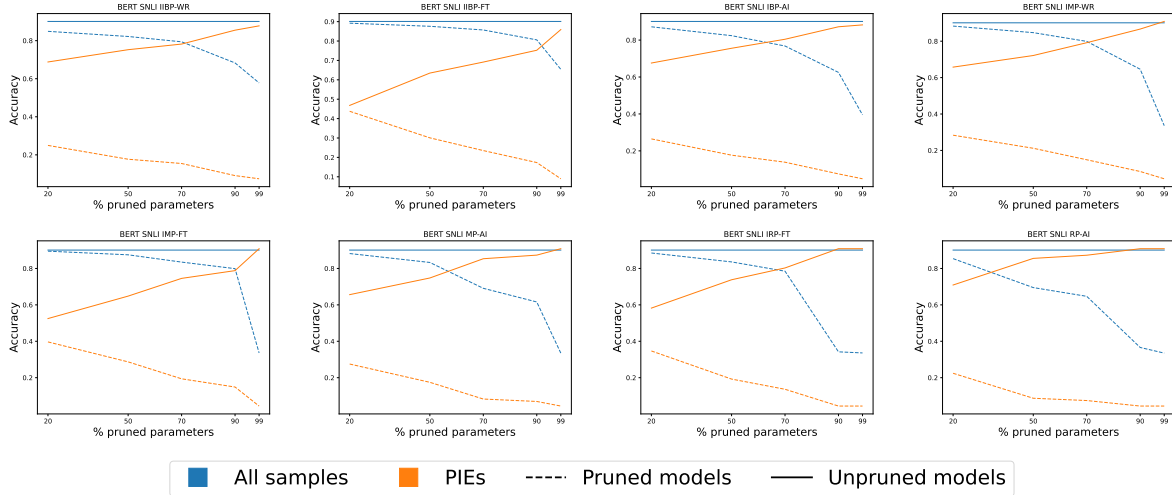


Figure 3: Accuracy (y axis) of unpruned (solid line) & pruned (dotted line) BERT on SNLI, for all data points (blue) or only for PIEs (orange), per pruning threshold (x axis), over 30 initializations. Each plot is a different pruner.

Figure 4 shows the distribution of PIEs across the degree of influence of all data points in the training set for IBP-FT (the rest of the plots are in Appendix B.2). We see that PIEs are concentrated among the most influential data points (right hand side of the plots). This is even more so for BERT, where up to 80% - 100% of its most influential data points are in fact PIEs, compared to up to 70% for BiLSTM. This explains the finding of Section 4.1 that BERT is more affected by pruning than BiLSTM, because (a) more influential examples are PIEs in BERT than in BiLSTM, and (b) accuracy/F1 is lower among PIEs than among all data points, as we saw in Figure 3. We conclude that **a considerable amount of those data points that have the largest influence on how well the model generalises to unseen data are PIEs.**

4.3 Textual characteristics of PIEs

The above findings motivate the need to understand what the text of PIEs actually looks like. We do this using the following eight scores of text readability and length: (1) Automated readability index (Senter and Smith, 1967); (2) Coleman-Liau index (Coleman and Liau, 1975); (3) Flesch-Kincaid grade level (Kincaid Jr et al., 1975); (4) Linsear Write (O’hayre, 1966); (5) Gunning Fog index (Gunning, 1969); (6) Dale-Chall readability (Dale and Chall, 1948); (7) Number of difficult words; and (8) Text length, counted as the number of tokens per text. (1)-(6) are different approximators of text readability in terms of what formal education level would be needed in order to understand

the text. (6) approximates comprehension difficulty based on a list of 3000 easily understandable words. (7) is a count of the number of words that are not in the Dale-Chall list of understandable words.

We compute the above scores first on all data points and then only on PIEs. Figure 5 shows the resulting plots for SNLI and BERT (the plots of the other configurations are in Appendix B.3). The black horizontal line represents all data points and PIEs having the same scores. Any divergence from this line reflects how much the scores of PIEs differ from those of all data points. E.g., the point 1.05 on the y axis of the Gunning Fog index plot means that the text of PIEs is approximately 1.05 times harder to understand than the text of all data points.

In Figure 5 we see that the formal education level needed for text understanding is overall higher for PIEs than for all data points (plots (a)-(e) and (g)). We also see that the text of PIEs has overall a larger amount of difficult words (plot (f)), and is on average longer than the text of all data points (plot (h)). Overall, according to the average scores of all pruning methods (turquoise line), PIE text is up to 1.03 times harder to understand than the text of all data points (plots (a)-(e) and (g)), with words that are up to 1.06 times more difficult (plot (f)), and text length that is up to 1.02 times longer (plot (h)). This means that **PIEs tend to be semantically more complex than the average text.** Note that the scores presented in plots (a)-(g) are designed to approximate human (as opposed to computational) difficulty in understanding text. This implies that **PIEs are more difficult than the average text,**

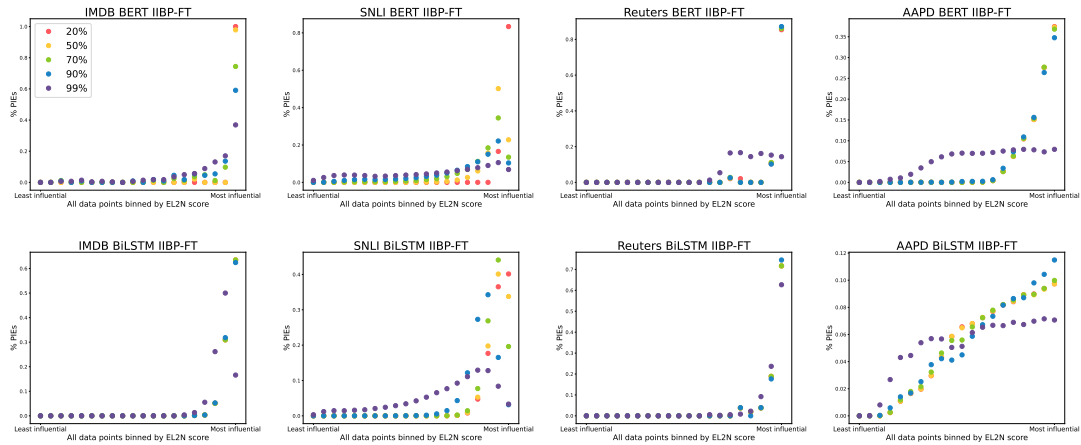


Figure 4: Percentage of data points that are PIEs (y axis) versus degree of influence (EL2N score) of all data points in the training set (x axis) for IIBP-FT across pruning thresholds (different colours).

397 **not only for LMs** (as shown in Figure 3), **but also**
 398 **for humans** (as shown in Figure 5).

399 5 Related work

400 **Pruning LMs.** LM pruning has typically been
 401 successful when models are first trained and then
 402 pruned (Li et al., 2020b). Most LM pruning meth-
 403 ods work either globally or locally (Zhu et al., 2023;
 404 Sun et al., 2023; Frantar and Alistarh, 2023). In the
 405 global case, entire neurons, layers, or even large
 406 sections of the LM are pruned simultaneously. Ex-
 407 amples include pruning entire attention heads in
 408 transformer models like BERT without severe infer-
 409 ence degradation (Michel et al., 2019), prun-
 410 ing entire blocks of layers with substantial effi-
 411 ciency gains and minimal effectiveness loss (La-
 412 gunas et al., 2021; Ma et al., 2024), or identifying
 413 a smaller sub-network, a "winning ticket", within
 414 a large model that can achieve performance compar-
 415 able to the original model when trained separ-
 416 ately (Yu et al., 2020; Prasanna et al., 2020). Such
 417 global compression methods can lead to more inter-
 418 pretable and manageable models, but have the dis-
 419 advantage that they tend to be architecture-specific.
 420 Unlike these global approaches, in local pruning,
 421 LM parameters/weights are pruned one layer at a
 422 time. This makes local pruning agnostic to partic-
 423 ular model architectures (LeCun et al., 1989),
 424 making it possible to compare the effect of prun-
 425 ing on different types of LMs. As a result, local
 426 pruning has been successfully applied in NLP (Zhu
 427 et al., 2023; Sun et al., 2023; Frantar and Alistarh,
 428 2023; Mishra and Chakraborty, 2021). In our study,
 429 we use only local pruning methods, allowing us to

study PIEs in both transformers and RNNs.

430
 431 For BERT in particular, it has been shown that
 432 a substantial amount of pruning can be applied
 433 during pre-training without significant loss in infer-
 434 ence (Sanh et al., 2020b). It has also been shown
 435 that specific parameters that are redundant to such
 436 transformer architectures can be accurately identi-
 437 fied by dedicated second-order pruning methods,
 438 such as Optimal BERT Surgeon (Frantar and Al-
 439 istarh, 2022). However, another body of recent
 440 work also shows that complex LM pruning meth-
 441 ods do not always work better than simpler, more
 442 straightforward pruning (Sun et al., 2024; Frantar
 443 and Alistarh, 2023).

444 Finally, researchers have also assessed, not only
 445 the accuracy, but also the loyalty (preservation of
 446 individual predictions) and robustness (resilience
 447 to adversarial attacks) of pruned BERT models (Xu
 448 et al., 2021). The findings reveal that traditional
 449 pruning methods that seem to maintain overall ac-
 450 curacy, may in fact affect the loyalty and robustness
 451 of the model. This line of work, similarly to ours,
 452 suggests that more nuanced analyses and evaluation
 453 approaches are needed to understand how pruning
 454 affects LMs beyond simple average accuracy.

455 **Impact of pruning on subsets of data.** While
 456 conventional pruned model evaluation has focused
 457 on inference time, number of pruned parameters,
 458 and effectiveness of the pruned models (Blalock
 459 et al., 2020; Gupta and Agrawal, 2022; Paganini
 460 and Forde, 2020; Renda et al., 2020), an under-
 461 studied aspect has been the impact of model prun-
 462 ing on subsets of data. As language data is often
 463 power distributed, pruning can have a more severe
 464 effect on the performance of the least frequent, tail

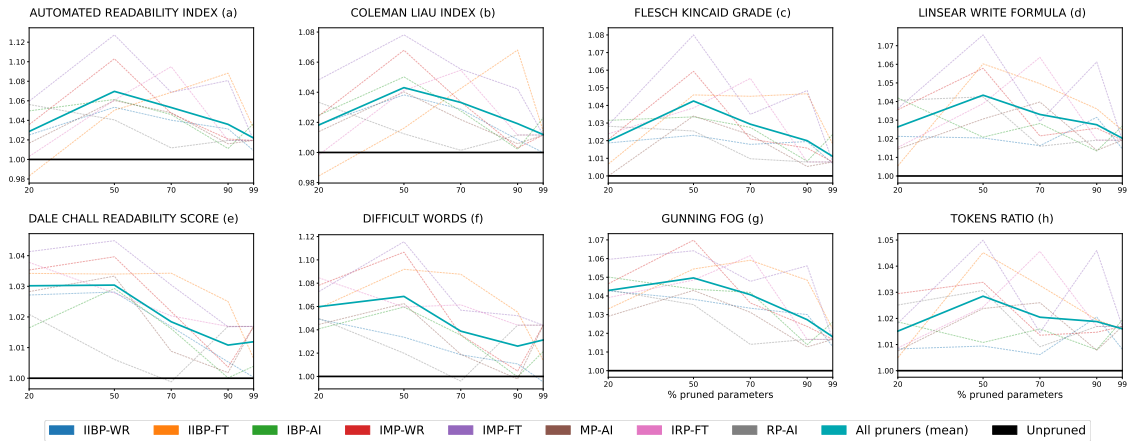


Figure 5: How the text of PIEs differs from the text of all data points, according to 7 readability scores (plots (a)-(g)) and text length (plot (h)). Ratio between the scores of PIEs and the scores of all data points (y axis), across pruning thresholds (x axis), for BERT and SNLI. The solid black horizontal line represents equal scores in PIEs and all data points. The solid turquoise line is the mean score of all pruners. Any line above the solid black line means that PIEs are harder to understand (plots (a)-(g)) or have longer text (plot (h)), on average, than all data points.

classes (Holste et al., 2023). This can make models less robust and more prone to overfit shortcuts (Du et al., 2023), result in disparate accuracy across subgroups of data (Tran et al., 2022; Hooker et al., 2020), and affect prediction quality based on sample frequency (Ogueji et al., 2022). Close to ours is the study of Hooker et al. (2019), who defined PIEs, and found them harder for both NNs and humans to classify. This study was limited to image processing. To our knowledge, our study is the first in-depth examination of PIEs for NLP, with novel findings about where and how often PIEs occur in text data, how they impact inference, and why.

6 Conclusions

We empirically studied how LMs are affected by pruning in the text domain. Unlike most work in this area which looks at overall gains in efficiency and costs to inference effectiveness, we zoomed in on precisely how pruning affects a particular subset of data points where pruned and unpruned models systematically disagree (*Pruning Identified Exemplars* (PIEs)). Using two LM architectures, four datasets, eight pruning methods, and five pruning thresholds, we found that PIEs impact inference quality considerably, but this effect goes undetected when reporting the mean accuracy across all data points. This effect is invariable to class frequency and increases the more we prune. BERT is overall more susceptible to this effect than BiLSTM. We also found that PIEs tend to contain a high amount of influential examples (data points that have the

largest influence on how well the model generalises to unseen data). Probing into what it is about PIEs that makes them both hard and impactful to inference, we found that their text is overall longer and more semantically complex, and harder to process not only for LMs but also for humans, based on human text readability approximations.

Overall, our findings suggest that, the more influential and complex a data instance is, the higher the chance that pruned and unpruned models will disagree on its prediction, impacting disproportionately a subset of the dataset, yet going generally unnoticed when reporting mean accuracy on the whole test set of data points. This can pose significant risks to LMs, such as focusing on easier examples, and sacrificing inference quality on more difficult examples that are however linked to better generalisation. Given the increased call for compressing LMs, pruning them without considering the effect to PIEs can make models vulnerable in high-stakes applications, where relying solely on good top-line performance is inadequate to guarantee the model’s reliability and trustworthiness across data instances and independently of class distribution.

Future work includes studying PIEs when pruning LLMs, and ways of balancing the impact of pruning fairly across PIEs and all data points.

Limitations

We evaluated the effects of pruning across eight pruning methods, two LM architectures, and four

527 datasets. While these are representative, we cannot
528 rule out the possibility that other pruning methods
529 or model architectures might yield different results.
530 Moreover, while we train BiLSTM from scratch,
531 BERT utilizes an existing backbone model. This
532 may affect some specific findings. Nonetheless,
533 our findings across all tested experimental condi-
534 tions, datasets, and models consistently point in
535 the same direction and unanimously support our
536 conclusions.

537 Future work could expand on our research by
538 exploring larger architectures and alternative prun-
539 ing methods. While we utilized extensive re-
540 sources from the LUMI supercomputing infrastruc-
541 ture (over 28000 AMD MI250X GPU hours), it was
542 not practically feasible to experiment with the lat-
543 est large language models in our setting where we
544 aimed varying many pruning thresholds, methods,
545 and datasets. However, future studies could investi-
546 gate individual architectures and pruning methods
547 in isolation and benchmark their results against our
548 findings.

549 We also did not explore the design of new prun-
550 ing algorithms that take into account properties of
551 the data, such as the link between the influence
552 of the examples and pruned and unpruned models
553 disagreement. These could help to mitigate both
554 general effectiveness drops as well as improved
555 handling of examples that are important for train-
556 ing and downstream usage of the models, which
557 we leave for future work.

558 Ethics Statement

559 We adhere to the ACM Code of Ethics and Pro-
560 fessional Conduct to ensure our work’s integrity,
561 fairness, and transparency.

562 Our study aims to enhance the understanding of
563 natural language model pruning. Our results re-
564 veal the trade-offs between performance and the
565 impact of pruning for examples that are potentially
566 lower frequency and minority class, but may be
567 highly important for downstream usage of the mod-
568 els. This can be particularly the case for high stakes
569 domains, such as fact checking, medical informat-
570 ics, and conversational and retrieval models that
571 can impact decisions and opinions of individuals.
572 By investigating the nuances of model pruning, we
573 aim to inform modeling practices that consider both
574 technical performance and potential weaknesses of
575 compressed models. This can be critical in many
576 specific application domains, but that is not always

577 accounted for in standard performance analysis fo-
578 cusing on average effectiveness. To this end, our
579 research identifies cases and settings where pruned
580 models may underperform, providing valuable in-
581 sights to avoid potential harm.

582 We have conducted our research fully transpar-
583 ently, documenting our methodologies and choices.
584 While our study did not involve human subjects
585 directly, it utilized publicly available datasets that
586 include human annotations. We ensured that the
587 use of these datasets complied with their respective
588 terms of use.

589 We have respected all intellectual property rights
590 in our research, and to our best knowledge prop-
591 erly citing all sources and datasets used. Our work
592 builds on existing literature while providing new
593 contributions to the field. We have also appropri-
594 ately acknowledged the contributions of other re-
595 searchers and sources that have informed our work.

596 We acknowledge that access to computing re-
597 sources can be a barrier for some researchers aim-
598 ing to reproduce our results. Our code to run the
599 models was trained with a LUMI supercomputer⁷,
600 available for academic use to reproduce the results.
601 We make our code and setup available to the scien-
602 tific audience for further validation by the research
603 community⁸.

Acknowledgements 604

References 605

- 606 Lukas Biewald. 2020. [Experiment tracking with](#)
607 [weights and biases](#). Software available from
608 [wandb.com](#).
- 609 Davis Blalock, Jose Javier Gonzalez Ortiz, Jonathan
610 Frankle, and John Gutttag. 2020. What is the state
611 of neural network pruning? *Proceedings of machine*
612 *learning and systems*, 2:129–146.
- 613 Samuel R. Bowman, Gabor Angeli, Christopher Potts,
614 and Christopher D. Manning. 2015. [A large anno-](#)
615 [tated corpus for learning natural language inference](#).
616 In *Proceedings of the 2015 Conference on Empiri-*
617 *cal Methods in Natural Language Processing*, pages
618 632–642, Lisbon, Portugal. Association for Compu-
619 tational Linguistics.
- 620 Tianlong Chen, Jonathan Frankle, Shiyu Chang, Sijia
621 Liu, Yang Zhang, Zhangyang Wang, and Michael
622 Carbin. 2020. The lottery ticket hypothesis for pre-
623 trained bert networks. *Advances in neural informa-*
624 *tion processing systems*, 33:15834–15846.

⁷<https://www.lumi-supercomputer.eu/>

⁸Code will be released upon acceptance

625	Meri Coleman and Ta Lin Liau. 1975. A computer readability formula designed for machine scoring. <i>Journal of Applied Psychology</i> , 60(2):283.	680
626		681
627		682
628	Edgar Dale and Jeanne S Chall. 1948. A formula for predicting readability: Instructions. <i>Educational research bulletin</i> , pages 37–54.	683
629		684
630		685
631	Jacob Devlin, Ming-Wei Chang, Kenton Lee, and Kristina Toutanova. 2019. BERT: pre-training of deep bidirectional transformers for language understanding . In <i>Proceedings of the 2019 Conference of the North American Chapter of the Association for Computational Linguistics: Human Language Technologies, NAACL-HLT 2019, Minneapolis, MN, USA, June 2-7, 2019, Volume 1 (Long and Short Papers)</i> , pages 4171–4186. Association for Computational Linguistics.	686
632		687
633		688
634		689
635		690
636		691
637		692
638		693
639		694
640		695
641	Mengnan Du, Subhabrata Mukherjee, Yu Cheng, Milad Shokouhi, Xia Hu, and Ahmed Hassan Awadallah. 2023. Robustness challenges in model distillation and pruning for natural language understanding . In <i>Proceedings of the 17th Conference of the European Chapter of the Association for Computational Linguistics</i> , pages 1766–1778, Dubrovnik, Croatia. Association for Computational Linguistics.	696
642		697
643		698
644		699
645		700
646		701
647		702
648		703
649	Mohsen Fayyaz, Ehsan Aghazadeh, Ali Modarressi, Mohammad Taher Pilehvar, Yadollah Yaghoobzadeh, and Samira Ebrahimi Kahou. 2022. Bert on a data diet: Finding important examples by gradient-based pruning. <i>arXiv preprint arXiv:2211.05610</i> .	704
650		705
651		706
652		707
653		708
654	Jonathan Frankle and Michael Carbin. 2019. The lottery ticket hypothesis: Finding sparse, trainable neural networks . In <i>7th International Conference on Learning Representations, ICLR 2019, New Orleans, LA, USA, May 6-9, 2019</i> . OpenReview.net.	709
655		710
656		711
657		712
658		713
659	Jonathan Frankle, Gintare Karolina Dziugaite, Daniel M. Roy, and Michael Carbin. 2021. Pruning neural networks at initialization: Why are we missing the mark? In <i>9th International Conference on Learning Representations, ICLR 2021, Virtual Event, Austria, May 3-7, 2021</i> . OpenReview.net.	714
660		715
661		716
662		717
663		718
664		719
665	Elias Frantar and Dan Alistarh. 2022. The optimal bert surgeon: Scalable and accurate second-order pruning for large language models . In <i>Proceedings of the 2022 Conference on Empirical Methods in Natural Language Processing (EMNLP)</i> , pages 10062–10079.	720
666		721
667		722
668		723
669		724
670		725
671	Elias Frantar and Dan Alistarh. 2023. Sparsegpt: Massive language models can be accurately pruned in one-shot . In <i>International Conference on Machine Learning</i> , pages 10323–10337. PMLR.	726
672		727
673		728
674		729
675	Robert Gunning. 1969. The fog index after twenty years. <i>Journal of Business Communication</i> , 6(2):3–13.	730
676		731
677	Manish Gupta and Puneet Agrawal. 2022. Compression of deep learning models for text: A survey . <i>ACM Trans. Knowl. Discov. Data</i> , 16(4):61:1–61:55.	732
678		733
679		734
		735
	Sepp Hochreiter and Jürgen Schmidhuber. 1997. Long short-term memory. <i>Neural computation</i> , 9(8):1735–1780.	
	Gregory Holste, Ziyu Jiang, Ajay Jaiswal, Maria Hanna, Shlomo Minkowitz, Alan C Legasto, Joanna G Escalon, Sharon Steinberger, Mark Bittman, Thomas C Shen, et al. 2023. How does pruning impact long-tailed multi-label medical image classifiers? In <i>International Conference on Medical Image Computing and Computer-Assisted Intervention</i> , pages 663–673. Springer.	
	Sara Hooker, Aaron Courville, Gregory Clark, Yann Dauphin, and Andrea Frome. 2019. What do compressed deep neural networks forget? <i>arXiv preprint arXiv:1911.05248</i> .	
	Sara Hooker, Nyalleng Moorosi, Gregory Clark, Samy Bengio, and Emily Denton. 2020. Characterising bias in compressed models. <i>arXiv preprint arXiv:2010.03058</i> .	
	Tian Jin, Michael Carbin, Dan Roy, Jonathan Frankle, and Gintare Karolina Dziugaite. 2022. Pruning’s effect on generalization through the lens of training and regularization. <i>Advances in Neural Information Processing Systems</i> , 35:37947–37961.	
	JP Kincaid Jr, Rogers Robert P Fishburne, L Chissom Richard, and S Brad. 1975. Derivation of new readability formulas (automated readability index, fog count and flesch reading ease formula) for navy enlisted personnel. (<i>No Title</i>).	
	François Lagunas, Ella Charlaix, Victor Sanh, and Alexander Rush. 2021. Block pruning for faster transformers . In <i>Proceedings of the 2021 Conference on Empirical Methods in Natural Language Processing</i> , pages 10619–10629, Online and Punta Cana, Dominican Republic. Association for Computational Linguistics.	
	Yann LeCun, John Denker, and Sara Solla. 1989. Optimal brain damage. <i>Advances in neural information processing systems</i> , 2.	
	Namhoon Lee, Thalaiyasingam Ajanthan, and Philip H. S. Torr. 2019. Snip: single-shot network pruning based on connection sensitivity . In <i>7th International Conference on Learning Representations, ICLR 2019, New Orleans, LA, USA, May 6-9, 2019</i> . OpenReview.net.	
	Zhuohan Li, Eric Wallace, Sheng Shen, Kevin Lin, Kurt Keutzer, Dan Klein, and Joey Gonzalez. 2020a. Train big, then compress: Rethinking model size for efficient training and inference of transformers . In <i>Proceedings of the 37th International Conference on Machine Learning</i> , volume 119 of <i>Proceedings of Machine Learning Research</i> , pages 5958–5968. PMLR.	
	Zhuohan Li, Eric Wallace, Sheng Shen, Kevin Lin, Kurt Keutzer, Dan Klein, and Joseph E. Gonzalez. 2020b. Train large, then compress: rethinking model size for	

736	efficient training and inference of transformers. In <i>Proceedings of the 37th International Conference on Machine Learning, ICML'20</i> . JMLR.org.	Alex Renda, Jonathan Frankle, and Michael Carbin. 2020. Comparing rewinding and fine-tuning in neural network pruning . In <i>8th International Conference on Learning Representations, ICLR 2020, Addis Ababa, Ethiopia, April 26-30, 2020</i> . OpenReview.net.	792
737			793
738			794
739	Xinyin Ma, Gongfan Fang, and Xinchao Wang. 2024. Llm-pruner: on the structural pruning of large language models. In <i>Proceedings of the 37th International Conference on Neural Information Processing Systems, NIPS '23</i> , Red Hook, NY, USA. Curran Associates Inc.	Victor Sanh, Thomas Wolf, and Alexander Rush. 2020a. Movement pruning: Adaptive sparsity by fine-tuning . In <i>Advances in Neural Information Processing Systems</i> , volume 33, pages 20378–20389. Curran Associates, Inc.	795
740			796
741			797
742			798
743			799
744			800
745	Andrew L. Maas, Raymond E. Daly, Peter T. Pham, Dan Huang, Andrew Y. Ng, and Christopher Potts. 2011. Learning word vectors for sentiment analysis . In <i>Proceedings of the 49th Annual Meeting of the Association for Computational Linguistics: Human Language Technologies</i> , pages 142–150, Portland, Oregon, USA. Association for Computational Linguistics.	Victor Sanh, Thomas Wolf, and Alexander M. Rush. 2020b. Compressing bert: Studying the effects of weight pruning on transfer learning . In <i>Proceedings of SustaiNLP: Workshop on Simple and Efficient Natural Language Processing</i> , pages 143–155.	801
746			802
747			803
748			804
749			805
750			806
751			807
752			808
753	Paul Michel, Omer Levy, and Graham Neubig. 2019. Are sixteen heads really better than one? In <i>Advances in Neural Information Processing Systems</i> , volume 32. Curran Associates, Inc.	RJ Senter and Edgar A Smith. 1967. Automated readability index. Technical report, Technical report, DTIC document.	809
754			810
755			811
756			812
757	Abhishek Kumar Mishra and Mohona Chakraborty. 2021. Does local pruning offer task-specific models to learn effectively? In <i>Proceedings of the Student Research Workshop Associated with RANLP 2021</i> , pages 118–125.	Mingjie Sun, Zhuang Liu, Anna Bair, and J Zico Kolter. 2023. A simple and effective pruning approach for large language models. In <i>The Twelfth International Conference on Learning Representations</i> .	813
758			814
759			815
760			816
761			817
762	Kelechi Ogueji, Orevaoghene Ahia, Gbemileke Onilude, Sebastian Gehrmann, Sara Hooker, and Julia Kreutzer. 2022. Intriguing properties of compression on multilingual models . In <i>Proceedings of the 2022 Conference on Empirical Methods in Natural Language Processing</i> , pages 9092–9110, Abu Dhabi, United Arab Emirates. Association for Computational Linguistics.	Mingjie Sun, Zhuang Liu, Anna Bair, and J. Zico Kolter. 2024. A simple and effective pruning approach for large language models.	818
763			819
764			820
765			821
766			822
767			823
768			824
769			825
770	John O'hayre. 1966. <i>Gobbledygook has gotta go</i> . US Department of the Interior, Bureau of Land Management.	Mingjie Sun, Zhuang Liu, Anna Bair, and J. Zico Kolter. 2020. Structured pruning of large language models . In <i>Proceedings of the 2020 Conference on Empirical Methods in Natural Language Processing (EMNLP)</i> , pages 6151–6162, Online. Association for Computational Linguistics.	826
771			827
772			828
773	Michela Paganini and Jessica Forde. 2020. On iterative neural network pruning, reinitialization, and the similarity of masks. <i>arXiv preprint arXiv:2001.05050</i> .	Thomas Wolf, Lysandre Debut, Victor Sanh, Julien Chaumond, Clement Delangue, Anthony Moi, Pierric Cistac, Tim Rault, Remi Louf, Morgan Funtowicz, Joe Davison, Sam Shleifer, Patrick von Platen, Clara Ma, Yacine Jernite, Julien Plu, Canwen Xu, Teven Le Scao, Sylvain Gugger, Mariama Drame, Quentin Lhoest, and Alexander Rush. 2020. Transformers: State-of-the-art natural language processing . In <i>Proceedings of the 2020 Conference on Empirical Methods in Natural Language Processing: System Demonstrations</i> , pages 38–45, Online. Association for Computational Linguistics.	829
774			830
775			831
776	Mansheej Paul, Surya Ganguli, and Gintare Karolina Dziugaite. 2021. Deep learning on a data diet: Finding important examples early in training. <i>Advances in Neural Information Processing Systems</i> , 34:20596–20607.		832
777			833
778			834
779			835
780			836
781	Jeffrey Pennington, Richard Socher, and Christopher D Manning. 2014. Glove: Global vectors for word representation. In <i>Proceedings of the 2014 conference on empirical methods in natural language processing (EMNLP)</i> , pages 1532–1543.		837
782			838
783			839
784			840
785			841
786	Sai Prasanna, Anna Rogers, and Anna Rumshisky. 2020. When BERT Plays the Lottery, All Tickets Are Winning . In <i>Proceedings of the 2020 Conference on Empirical Methods in Natural Language Processing (EMNLP)</i> , pages 3208–3229, Online. Association for Computational Linguistics.	Canwen Xu, Kaitao Song, Xu Tan, Tao Qin, Jianfeng Lu, and Tie-Yan Liu. 2021. Beyond preserved accuracy: Evaluating loyalty and robustness of bert compression . In <i>Proceedings of the 2021 Conference on Empirical Methods in Natural Language Processing (EMNLP)</i> , pages 10590–10600.	842
787			843
788			844
789			
790			
791			

Pengcheng Yang, Xu Sun, Wei Li, Shuming Ma, Wei Wu, and Houfeng Wang. 2018. Sgm: Sequence generation model for multi-label classification. In *Proceedings of the 27th International Conference on Computational Linguistics*, pages 3915–3926.

Haonan Yu, Sergey Edunov, Yuandong Tian, and Ari S. Morcos. 2020. *Playing the lottery with rewards and multiple languages: lottery tickets in RL and NLP*. In *8th International Conference on Learning Representations, ICLR 2020, Addis Ababa, Ethiopia, April 26-30, 2020*. OpenReview.net.

Xunyu Zhu, Jian Li, Yong Liu, Can Ma, and Weiping Wang. 2023. A survey on model compression for large language models. *arXiv preprint arXiv:2308.07633*.

A Implementation Details

A.1 Language Model Architectures

We use the pretrained uncased version of BERT-base from HuggingFace as is, which has 12 encoders with 12 self-attention heads (Wolf et al., 2020). BERT takes as input the tokenized text. We set the output layer size to match the number of classes of the data set the model is trained on. During training, we tune all of BERT’s parameters

Our BiLSTM models receive as input a vector representation of the words in the text. To build such a vector we use Glove embeddings of size 300 (Pennington et al., 2014). We input the embeddings to a multilayer BiLSTM. We set the output layer size of the BiLSTM models to match the number of classes of the data set the model is trained on. On BiLSTM, we always use rectified linear units (ReLU) as activation functions.

We present the “percentage of pruned parameters” based on the total number of parameters that can be pruned in the model, instead of all of the parameters of the model (Chen et al., 2020). In Table 5 and Table 6 we report information about the number of remaining parameters in the architectures at different pruning amounts.

A.2 Datasets and Preprocessing

In table 7 we report dataset statistics after preprocessing. IMDB (Maas et al., 2011) is a single-label sentiment analysis dataset, made of reviews of movies. Each review is either positive or negative. IMDB has the longest sentences and the fewest classes across all our datasets on average. SNLI is a single-label natural language inference dataset. Each sample contains two sentences, and the task is to determine if the relationship between them is entailment, contradiction, or neutral. The dataset is

LM	Dataset	# parameters	20%	50%	70%	90%	99%
BERT	IMDB	109,483,778					
	SNLI	109,484,547	15%	39%	55%	70%	77%
	Reuters	109,499,927					
	AAPD	109,523,766					
BiLSTM	IMDB	647,810					
	SNLI	647,939	20%	50%	69%	89%	98%
	Reuters	650,519					
	AAPD	654,518					

Table 5: Number of LM parameters and % of parameters that are removed when pruning at 20%–99%. Numbers differ per dataset because the different size of the classification layer leads LMs to a different final amount of parameters.

Architecture	Unpruned	20	50	70	90	99
BERT	1.1×10^8	9.2×10^7	6.7×10^7	5.0×10^7	3.2×10^7	2.5×10^7
BiLSTM	6.5×10^5	5.2×10^5	3.3×10^5	2.0×10^5	6.8×10^4	1.0×10^4

Table 6: Number of parameters for the unpruned models, and remaining parameters when pruning at 20%-99%.

available under a CC BY-SA license. SNLI has the most training samples and the shortest sentences among all our datasets on average. Reuters-21578 is a multi-label document categorization dataset, made of Reuters news belonging to 120 topics. Each news item is categorized and can belong to multiple topics. After preprocessing, the dataset has 23 classes. The dataset is available under CC BY license. Reuters has the fewest training samples among our datasets. AAPD is a multi-label document categorization dataset of article abstracts in computer science. Each article can belong to multiple subjects, and the task is to identify the subjects given the abstract. The dataset is available under CC BY license. AAPD has the most classes across our datasets.

Dataset preprocessing. IMDB has 25000 training examples and 25000 test examples. To perform hyperparameter tuning of our models, we apply stratified sampling from the original training set to create a validation set of 5000 samples. On SNLI we use the original data set splits. On Reuters-21578 we remove all of the topics that do not appear in at least 100 documents and all of the documents that do not belong to at least one of the remaining topics. We perform stratified sampling and create three partitions by allocating 30% of the samples to the training set, 15% to the validation set, and 15% to the test set. For computational efficiency, before computing the statistics shown in Table 7, we convert texts in the Reuters dataset to lowercase and remove punctuation and numbers. Lastly, we use the original splits for the AAPD data set.

We further pad and truncate texts to submit train-

Dataset	# train	# test	# val	Mean/median	Min/max len	Std len	Tokens 85%	Max tokens	# classes	Task	Classification
IMDB	20000	25000	5000	268/201	8/2753	197	430	512	2	Sentiment analysis	single-label
SNLI	549367	9824	9842	23/22	5/124	7	30	128	3	Natural language inference	single-label
Reuters	6737	1429	1440	126/79	5/1305	137	232	256	23	Document categorization	multi-label
AAPD	53840	1000	1000	167/161	1/599	70	242	256	54	Document categorization	multi-label

Table 7: Datasets’ statistics after preprocessing. # train, # test, and # val are respectively the number of instances in train, test, and validation sets. Mean/median, and Min/max are respectively the mean, median, minimum, and maximum number of tokens in the dataset’s instances. Tokens 85% represent a value such that 85% of the datasets’ texts have fewer or equal tokens than such value. Max tokens are the number of tokens, starting from the beginning of the text, after which we truncate texts. # classes is the number of classes. Task is the task solved using the dataset.

ing examples in batches, and we select a strategy to handle terms that are not present in the model’s vocabulary (OOV). We explain these two steps next.

To fully take advantage of the available hardware, we submit training examples to the models in batches. When multiple texts with a different amount of tokens are present in a batch, our models require padding on the shorter texts in such a way that each input has the same amount of tokens. To have batches where each text is of equal size, we truncate long texts and pad short ones. Note that we do not remove documents based on a minimum amount of tokens in the text. To truncate the texts, we find a threshold after which we perform truncation. We define this threshold as the first power of two after which, by selecting the value as a threshold, at least 85% of the texts in the dataset do not need to be truncated. The resulting thresholds are reported as “Max tokens” in Table 7. An exception is made for SNLI. The SNLI dataset is made of short texts, and even the longest text is under 128 tokens. Hence we consider 128 tokens, representing the whole text for each sample in the data set. We then proceed to pad short texts in each batch to always exactly match the number of tokens specified in Table 7. For BERT we use the huggingface’s tokenizer padding and pad all of the texts in each dataset to the respective “Max tokens” value in Table 7. BERT will mask and ignore the padding. For the BiLSTM model, we represent padding as a randomly generated embedding according to the mean and std distribution in Glove.

On BERT, OOV terms are assigned the default UNK token. On BiLSTM, we represent OOV terms with a vector defined as the average over all of the present word embeddings. The result of our preprocessing will be texts with exactly “Max tokens” tokens in which OOV terms are represented by the

UNK token on BERT and as the average embedding vector on BiLSTM.

A.3 Pruning Methods

Model parameters are pruned one layer at a time. We prune uniformly across layers, i.e. we remove the same percentage of parameters in each layer. Following Chen et al. (2020) and Yu et al. (2020); Prasanna et al. (2020), we do not prune embedding layers and biases of the LMs (Gupta and Agrawal, 2022). We also do not prune the final classification layer, because its weights are likely disproportionately important to reach high effectiveness (Frankle et al., 2021).

With iterative pruning, we select a pruning percentage and keep it fixed for each pruning iteration to reach our pruning goal in exactly three iterations across all datasets, LMs, and pruning percentages. We train the model (BERT or BiLSTM) fully for N epochs, prune according to the selected percentage, and then retrain for N epochs. This process repeats until we achieve our pruning target as per (Jin et al., 2022). In total, this procedure requires four times the training iterations when compared to pruning at initialization.

A.4 Hyperparameter Tuning

We tune the unpruned model’s hyperparameters for each combination of architecture and dataset. The resulting hyperparameters are then used to train both unpruned and pruned models. We do not tune hyperparameters of the pruning algorithms. The only tunable aspect when pruning at initialization is the percentage of parameters to prune. However, in our experiments, we fix five different values for this hyperparameter and we test such values on all pruning algorithms, hence, we do not optimize the percentage of pruned parameters. When pruning iteratively (with or without weight rewinding)

Dataset	Architecture	Batch size	Epochs		Best epoch	lr		Best lr
			Min	Max		Min	Max	
IMDB	BERT	32	2	6	3	2e-5	2e-4	0.00007
	BILSTM	1024	10	30	26	2e-4	2e-3	0.00196
SNLI	BERT	256	2	6	2	2e-5	2e-4	0.00014
	BILSTM	4096	30	50	39	2e-4	2e-3	0.00180
Reuters	BERT	128	5	15	14	2e-5	2e-4	0.00016
	BILSTM	512	30	100	72	2e-4	2e-3	0.00152
AAPD	BERT	256	5	15	13	2e-5	2e-4	0.00015
	BILSTM	2048	30	60	50	2e-4	2e-3	0.00184

Table 8: Search space and best configuration for the hyperparameter tuning of the models. Min and Max epochs represent the range of epochs used to perform hyperparameter tuning. Best epoch is the best epoch found with hyperparameter tuning. Min and Max lr are the range learning rate is tuned on. Best lr is the best learning rate found during hyperparameter optimization. The batch size is set to maximize the GPU usage.

we also need to select the number of pruning iterations and the amount of parameters to prune at each pruning iteration. To allow for comparison between pruning algorithms, we select a fixed percentage of parameters to remove during each iteration, such that in exactly 3 iterations the desired amount of parameters will be pruned. Hence those hyperparameters are inferred and fixed in each setting, leaving no hyperparameters to be optimized when pruning iteratively.

The hyperparameter tuning is performed separately on architectures and separately for each data set. We tune the hyperparameters using the random optimization from the weights and biases (WandB) platform with a budget of 100 objective function evaluations (Biewald, 2020). Hyperparameter tuning is set to maximize accuracy and macro F1 in the validation set for the single-label and multi-label tasks respectively. The search spaces optimal hyperparameter values are summarized in Table 8.

B Results

In Table 3 we report accuracy and F1 score with their standard deviation, obtained by unpruned models and pruned models at different amounts of pruned parameters.

In Table 10 we report accuracy and F1 score on PIEs obtained by unpruned models and pruned models at different amounts of pruned parameters. We highlight in blue the cases where the pruned models are on average more effective than the unpruned models on PIEs.

B.1 Pruning and occurrence of PIEs

We report here the additional results of Section 4.1.

In Figure 6 we show the distribution of all data points and of PIEs at 20% to 99% pruning, across

classes sorted by frequency for the multi-label datasets. We observe the same overall trend in all settings. Regardless of the language model architecture, the percentage of PIEs in the most frequent class for Reuters is much lower than the percentage of examples belonging to the same class in all data points. This means that the disagreement between pruned and unpruned models is not focused on the most frequent class of Reuters. The disagreement is skewed instead towards the less frequent classes. On AAPD we observe a similar behaviour, however, the percentage of PIEs belonging to the most frequent class is higher, hence the disagreement is slightly more balanced across all classes.

In Figures 7, 8, 9, 10, 11, 12, and 13 we report the accuracy of unpruned and pruned models on PIEs and all samples in the dataset per pruning method, across pruning thresholds. The accuracy on PIEs is lower than the accuracy on all data points for both pruned and unpruned models. The accuracy of the unpruned model on PIEs increases when increasing the amount of pruned parameters, while the accuracy of the pruned model decreases in the same setting. This is because the pruned model misclassifies more samples that are correctly classified by the unpruned model, increasing the amount of disagreement, hence the number of PIEs too.

B.2 Influential examples in PIEs

We report here the additional results of Section 4.2. Figures 14, 15, 16, 17, 18, 19, and 20 report the percentage of data points that are PIEs versus the degree of influence of all data points in the training set, for each pruning algorithm. PIEs are concentrated on the most influential examples. The higher the amount of pruned parameters, the more PIEs are distributed across examples with different influence on model generalization.

B.3 Textual characteristics of PIEs

We report here the additional results of Section 4.3.

In most cases, the formal education level needed to understand PIEs is higher than for all data points, with the exception of AAPD. AAPD leads to significant disagreement between pruned and unpruned models, even with 20% parameter pruning (See Table 4)). This is due to our extension of PIEs for multi-label settings, which considers a sample as a PIE if there is prediction disagreement on any class. The more classes in the dataset, the higher the chance of samples being labelled as PIEs. AAPD has 53 classes, the highest class count of

			Single-label: Accuracy						
% pruned parameters			0%	20%	50%	70%	90%	99%	
dataset	model	pruning algo							
IMDB	BERT	IIBP-WR	.932 ± .005	.892 ± .009	.870 ± .016	.864 ± .026	.863 ± .011	.742 ± .136	
		IIBP-FT	.932 ± .005	.919 ± .004	.869 ± .008	.848 ± .007	.843 ± .010	.828 ± .064	
		IBP-AI	.932 ± .005	.882 ± .010	.864 ± .021	.865 ± .016	.841 ± .069	.526 ± .079	
		IMP-WR	.932 ± .005	.911 ± .009	.880 ± .006	.870 ± .009	.857 ± .007	.500 ± .000	
		IMP-FT	.932 ± .005	.924 ± .004	.873 ± .007	.845 ± .004	.850 ± .007	.500 ± .000	
		MP-AI	.932 ± .005	.904 ± .008	.871 ± .009	.867 ± .010	.852 ± .011	.500 ± .000	
		IRP-FT	.932 ± .005	.877 ± .011	.846 ± .009	.778 ± .141	.500 ± .000	.500 ± .000	
		RP-AI	.932 ± .005	.874 ± .004	.866 ± .012	.828 ± .114	.500 ± .000	.500 ± .000	
	BiLSTM	IIBP-WR	.879 ± .016	.868 ± .021	.861 ± .026	.856 ± .027	.837 ± .025	.806 ± .026	
		IIBP-FT	.879 ± .016	.883 ± .011	.880 ± .013	.878 ± .010	.872 ± .011	.872 ± .013	
		IBP-AI	.879 ± .016	.874 ± .017	.848 ± .019	.820 ± .032	.805 ± .029	.755 ± .022	
		IMP-WR	.879 ± .016	.875 ± .020	.881 ± .012	.876 ± .011	.873 ± .025	.804 ± .018	
		IMP-FT	.879 ± .016	.886 ± .010	.887 ± .010	.882 ± .009	.878 ± .007	.862 ± .013	
		MP-AI	.879 ± .016	.872 ± .019	.855 ± .018	.843 ± .023	.834 ± .015	.755 ± .021	
		IRP-FT	.879 ± .016	.885 ± .010	.875 ± .011	.875 ± .012	.873 ± .017	.548 ± .073	
		RP-AI	.879 ± .016	.872 ± .037	.848 ± .027	.845 ± .026	.840 ± .016	.721 ± .024	
SNLI	BERT	IIBP-WR	.901 ± .002	.849 ± .098	.822 ± .004	.794 ± .007	.683 ± .044	.578 ± .053	
		IIBP-FT	.901 ± .002	.892 ± .002	.876 ± .003	.857 ± .003	.806 ± .090	.654 ± .071	
		IBP-AI	.901 ± .002	.872 ± .002	.824 ± .005	.768 ± .028	.625 ± .016	.395 ± .086	
		IMP-WR	.901 ± .002	.883 ± .003	.847 ± .004	.799 ± .004	.646 ± .033	.336 ± .008	
		IMP-FT	.901 ± .002	.895 ± .002	.875 ± .002	.835 ± .004	.799 ± .005	.336 ± .008	
		MP-AI	.901 ± .002	.882 ± .002	.833 ± .003	.691 ± .016	.616 ± .011	.335 ± .007	
		IRP-FT	.901 ± .002	.885 ± .003	.836 ± .004	.785 ± .008	.342 ± .034	.336 ± .008	
		RP-AI	.901 ± .002	.854 ± .004	.695 ± .007	.647 ± .005	.366 ± .069	.335 ± .007	
	BiLSTM	IIBP-WR	.778 ± .004	.780 ± .004	.774 ± .005	.763 ± .005	.715 ± .007	.614 ± .007	
		IIBP-FT	.778 ± .004	.742 ± .004	.750 ± .004	.762 ± .003	.771 ± .004	.657 ± .011	
		IBP-AI	.778 ± .004	.776 ± .004	.766 ± .004	.743 ± .007	.669 ± .009	.431 ± .104	
		IMP-WR	.778 ± .004	.779 ± .004	.782 ± .004	.782 ± .004	.726 ± .009	.336 ± .007	
		IMP-FT	.778 ± .004	.741 ± .004	.746 ± .004	.766 ± .003	.765 ± .004	.574 ± .019	
		MP-AI	.778 ± .004	.776 ± .004	.764 ± .006	.743 ± .005	.687 ± .007	.336 ± .007	
		IRP-FT	.778 ± .004	.746 ± .004	.769 ± .004	.779 ± .004	.712 ± .007	.389 ± .070	
		RP-AI	.778 ± .004	.776 ± .003	.762 ± .005	.739 ± .006	.667 ± .017	.336 ± .007	
			Multi-label: F1 Macro						
% pruned parameters			0%	20%	50%	70%	90%	99%	
dataset	model	pruning algo							
Reuters	BERT	IIBP-WR	.836 ± .004	.822 ± .011	.792 ± .018	.674 ± .064	.382 ± .046	.167 ± .041	
		IIBP-FT	.836 ± .004	.835 ± .005	.830 ± .005	.822 ± .008	.786 ± .029	.355 ± .061	
		IBP-AI	.836 ± .004	.810 ± .008	.645 ± .048	.328 ± .048	.189 ± .027	.096 ± .018	
		IMP-WR	.836 ± .004	.827 ± .006	.829 ± .005	.736 ± .015	.147 ± .025	.082 ± .008	
		IMP-FT	.836 ± .004	.838 ± .005	.834 ± .005	.824 ± .006	.490 ± .086	.085 ± .005	
		MP-AI	.836 ± .004	.822 ± .006	.745 ± .021	.417 ± .057	.127 ± .031	.086 ± .004	
		IRP-FT	.836 ± .004	.832 ± .005	.769 ± .013	.524 ± .075	.087 ± .001	.087 ± .002	
		RP-AI	.836 ± .004	.803 ± .007	.479 ± .052	.242 ± .021	.089 ± .012	.086 ± .003	
	BiLSTM	IIBP-WR	.731 ± .017	.728 ± .018	.727 ± .016	.716 ± .014	.631 ± .036	.396 ± .040	
		IIBP-FT	.731 ± .017	.753 ± .018	.751 ± .013	.751 ± .015	.742 ± .014	.693 ± .019	
		IBP-AI	.731 ± .017	.729 ± .020	.706 ± .019	.616 ± .029	.456 ± .036	.224 ± .028	
		IMP-WR	.731 ± .017	.726 ± .017	.738 ± .015	.745 ± .012	.734 ± .011	.481 ± .032	
		IMP-FT	.731 ± .017	.751 ± .013	.747 ± .014	.745 ± .017	.746 ± .012	.657 ± .028	
		MP-AI	.731 ± .017	.740 ± .012	.730 ± .014	.705 ± .022	.606 ± .026	.393 ± .034	
		IRP-FT	.731 ± .017	.753 ± .015	.757 ± .015	.760 ± .014	.743 ± .012	.417 ± .042	
		RP-AI	.731 ± .017	.731 ± .019	.724 ± .015	.661 ± .028	.570 ± .030	.377 ± .042	
AAPD	BERT	IIBP-WR	.578 ± .007	.547 ± .008	.518 ± .009	.482 ± .010	.403 ± .018	.179 ± .032	
		IIBP-FT	.578 ± .007	.573 ± .009	.548 ± .009	.462 ± .153	.476 ± .018	.316 ± .033	
		IBP-AI	.578 ± .007	.539 ± .009	.480 ± .015	.398 ± .023	.234 ± .042	.091 ± .016	
		IMP-WR	.578 ± .007	.567 ± .009	.541 ± .007	.483 ± .008	.230 ± .029	.080 ± .001	
		IMP-FT	.578 ± .007	.579 ± .009	.546 ± .008	.521 ± .008	.400 ± .019	.080 ± .000	
		MP-AI	.578 ± .007	.551 ± .008	.508 ± .010	.423 ± .014	.145 ± .007	.080 ± .000	
		IRP-FT	.578 ± .007	.554 ± .009	.312 ± .197	.338 ± .133	.082 ± .014	.080 ± .000	
		RP-AI	.578 ± .007	.524 ± .009	.397 ± .015	.261 ± .029	.082 ± .007	.080 ± .000	
	BiLSTM	IIBP-WR	.468 ± .015	.449 ± .022	.441 ± .022	.444 ± .020	.346 ± .022	.163 ± .028	
		IIBP-FT	.468 ± .015	.429 ± .013	.425 ± .015	.436 ± .009	.486 ± .010	.396 ± .012	
		IBP-AI	.468 ± .015	.473 ± .014	.459 ± .011	.398 ± .029	.190 ± .027	.082 ± .004	
		IMP-WR	.468 ± .015	.446 ± .018	.454 ± .016	.454 ± .013	.406 ± .014	.185 ± .019	
		IMP-FT	.468 ± .015	.428 ± .014	.421 ± .013	.432 ± .015	.486 ± .009	.330 ± .020	
		MP-AI	.468 ± .015	.473 ± .015	.473 ± .010	.454 ± .011	.385 ± .020	.165 ± .025	
		IRP-FT	.468 ± .015	.432 ± .012	.451 ± .013	.486 ± .012	.475 ± .010	.167 ± .025	
		RP-AI	.468 ± .015	.464 ± .014	.453 ± .018	.421 ± .023	.356 ± .021	.163 ± .025	

Table 9: Average macro accuracy/F1 score and std over 30 model initializations. Pruning algo is the used pruning algorithm according to Table 3. The best results for each percentage of pruned parameters and combination of dataset and architecture are in bold.

		Single-label										
		Pruner	20%		50%		70%		90%		99%	
IMDB	BERT	IIBP-WR	0.245	0.755	0.200	0.800	0.191	0.809	0.188	0.812	0.182	0.818
		IIBP-FT	0.356	0.644	0.195	0.805	0.161	0.839	0.163	0.837	0.188	0.812
		IBP-AI	0.227	0.773	0.195	0.805	0.198	0.802	0.205	0.795	0.056	0.944
		IMP-WR	0.290	0.710	0.206	0.794	0.194	0.806	0.179	0.821	0.056	0.944
		IMP-FT	0.385	0.615	0.200	0.800	0.156	0.844	0.167	0.833	0.056	0.944
	BiLSTM	MP-AI	0.262	0.738	0.197	0.803	0.192	0.808	0.180	0.820	0.056	0.944
		IRP-FT	0.220	0.780	0.161	0.839	0.172	0.828	0.056	0.944	0.056	0.944
		RP-AI	0.198	0.802	0.199	0.801	0.198	0.802	0.056	0.944	0.056	0.944
		IIBP-WR	0.371	0.629	0.322	0.678	0.283	0.717	0.232	0.768	0.207	0.793
		IIBP-FT	0.604	0.396	0.616	0.384	0.598	0.402	0.555	0.445	0.471	0.529
SNLI	BERT	IBP-AI	0.382	0.618	0.253	0.747	0.209	0.791	0.206	0.794	0.168	0.832
		IMP-WR	0.471	0.529	0.542	0.458	0.480	0.520	0.470	0.530	0.218	0.782
		IMP-FT	0.644	0.356	0.658	0.342	0.584	0.416	0.613	0.387	0.395	0.605
		MP-AI	0.404	0.596	0.281	0.719	0.241	0.759	0.225	0.775	0.178	0.822
		IRP-FT	0.633	0.367	0.577	0.423	0.576	0.424	0.404	0.596	0.126	0.874
	BiLSTM	RP-AI	0.403	0.597	0.269	0.731	0.250	0.750	0.230	0.770	0.161	0.839
		IIBP-WR	0.250	0.688	0.177	0.753	0.155	0.782	0.091	0.855	0.074	0.878
		IIBP-FT	0.438	0.468	0.301	0.635	0.235	0.692	0.173	0.752	0.090	0.859
		IBP-AI	0.265	0.676	0.177	0.756	0.139	0.805	0.075	0.872	0.049	0.882
		IMP-WR	0.284	0.658	0.212	0.721	0.149	0.792	0.084	0.867	0.044	0.909
AAPD	BERT	IMP-FT	0.397	0.525	0.287	0.648	0.194	0.746	0.149	0.788	0.044	0.909
		MP-AI	0.275	0.656	0.175	0.748	0.083	0.853	0.069	0.873	0.044	0.909
		IRP-FT	0.347	0.582	0.192	0.738	0.136	0.803	0.044	0.909	0.044	0.909
		RP-AI	0.224	0.709	0.087	0.855	0.074	0.873	0.044	0.909	0.044	0.909
		IIBP-WR	0.445	0.464	0.356	0.549	0.278	0.618	0.208	0.682	0.153	0.750
	BiLSTM	IIBP-FT	0.467	0.413	0.529	0.366	0.517	0.368	0.391	0.493	0.184	0.719
		IBP-AI	0.382	0.518	0.298	0.582	0.258	0.626	0.177	0.722	0.124	0.760
		IMP-WR	0.434	0.454	0.461	0.429	0.447	0.451	0.225	0.670	0.068	0.824
		IMP-FT	0.495	0.381	0.496	0.379	0.522	0.361	0.375	0.522	0.141	0.758
		MP-AI	0.397	0.490	0.296	0.596	0.247	0.640	0.196	0.705	0.068	0.824
Reuters	BERT	IRP-FT	0.512	0.389	0.535	0.340	0.498	0.393	0.215	0.677	0.101	0.796
		RP-AI	0.371	0.524	0.281	0.620	0.243	0.649	0.175	0.728	0.068	0.824
		IIBP-WR	0.575	0.620	0.561	0.664	0.545	0.777	0.319	0.807	0.167	0.837
		IIBP-FT	0.608	0.591	0.572	0.567	0.589	0.621	0.530	0.659	0.302	0.820
		IBP-AI	0.572	0.656	0.506	0.780	0.276	0.825	0.182	0.838	0.096	0.836
	BiLSTM	IMP-WR	0.563	0.602	0.529	0.570	0.545	0.726	0.147	0.837	0.082	0.836
		IMP-FT	0.619	0.602	0.555	0.596	0.590	0.627	0.393	0.794	0.085	0.836
		MP-AI	0.555	0.610	0.555	0.743	0.359	0.819	0.127	0.836	0.086	0.836
		IRP-FT	0.604	0.621	0.530	0.714	0.422	0.806	0.087	0.836	0.087	0.836
		RP-AI	0.560	0.666	0.428	0.815	0.196	0.825	0.089	0.836	0.086	0.836
AAPD	BERT	IIBP-WR	0.466	0.462	0.498	0.500	0.483	0.509	0.509	0.620	0.362	0.701
		IIBP-FT	0.476	0.423	0.490	0.440	0.511	0.442	0.508	0.432	0.496	0.509
		IBP-AI	0.452	0.459	0.489	0.529	0.501	0.620	0.422	0.708	0.193	0.720
		IMP-WR	0.464	0.470	0.445	0.448	0.483	0.451	0.521	0.485	0.435	0.696
		IMP-FT	0.519	0.462	0.521	0.452	0.504	0.443	0.526	0.447	0.496	0.577
	BiLSTM	MP-AI	0.495	0.470	0.472	0.478	0.514	0.557	0.504	0.638	0.356	0.711
		IRP-FT	0.500	0.423	0.480	0.399	0.488	0.416	0.512	0.440	0.375	0.704
		RP-AI	0.453	0.446	0.510	0.517	0.510	0.593	0.507	0.676	0.346	0.710
		IIBP-WR	0.471	0.511	0.453	0.529	0.432	0.553	0.367	0.563	0.175	0.580
		IIBP-FT	0.498	0.506	0.476	0.515	0.417	0.542	0.418	0.556	0.292	0.576
AAPD	BERT	IBP-AI	0.463	0.515	0.430	0.548	0.366	0.566	0.229	0.582	0.091	0.578
		IMP-WR	0.492	0.507	0.475	0.525	0.428	0.552	0.225	0.582	0.080	0.578
		IMP-FT	0.502	0.506	0.484	0.532	0.462	0.537	0.366	0.569	0.080	0.578
		MP-AI	0.475	0.517	0.452	0.544	0.390	0.568	0.143	0.579	0.080	0.578
		IRP-FT	0.483	0.519	0.295	0.560	0.311	0.565	0.082	0.578	0.080	0.578
	BiLSTM	RP-AI	0.448	0.516	0.364	0.568	0.255	0.583	0.082	0.578	0.080	0.578
		IIBP-WR	0.391	0.416	0.405	0.443	0.413	0.445	0.333	0.461	0.160	0.469
		IIBP-FT	0.393	0.439	0.380	0.430	0.388	0.424	0.432	0.413	0.380	0.459
		IBP-AI	0.402	0.392	0.410	0.422	0.378	0.454	0.184	0.468	0.082	0.468
		IMP-WR	0.399	0.427	0.397	0.417	0.421	0.441	0.383	0.453	0.180	0.469
BiLSTM	IMP-FT	0.389	0.435	0.375	0.432	0.386	0.432	0.442	0.425	0.318	0.462	
	MP-AI	0.393	0.385	0.434	0.430	0.421	0.439	0.365	0.457	0.162	0.469	
	IRP-FT	0.386	0.431	0.413	0.429	0.436	0.411	0.448	0.439	0.164	0.468	
	RP-AI	0.411	0.417	0.409	0.432	0.397	0.451	0.344	0.462	0.160	0.470	

Table 10: Average pruned and unpruned models’ effectiveness on PIEs when pruning 20, 50, 70, 90, and 99% of the parameters. For each pruning percentage column, the first value refers to the effectiveness of the pruned models on PIEs, the second value represents the effectiveness of the unpruned models on the same set of PIEs. We represent models’ effectiveness through accuracy in Single-label and F1 macro in Multi-label settings. The blue colour identifies cases where the pruned models have higher effectiveness on PIEs than the unpruned ones. We represent in bold the cases where the effectiveness of the models on PIEs is higher than the effectiveness of the same models on the whole dataset instead.

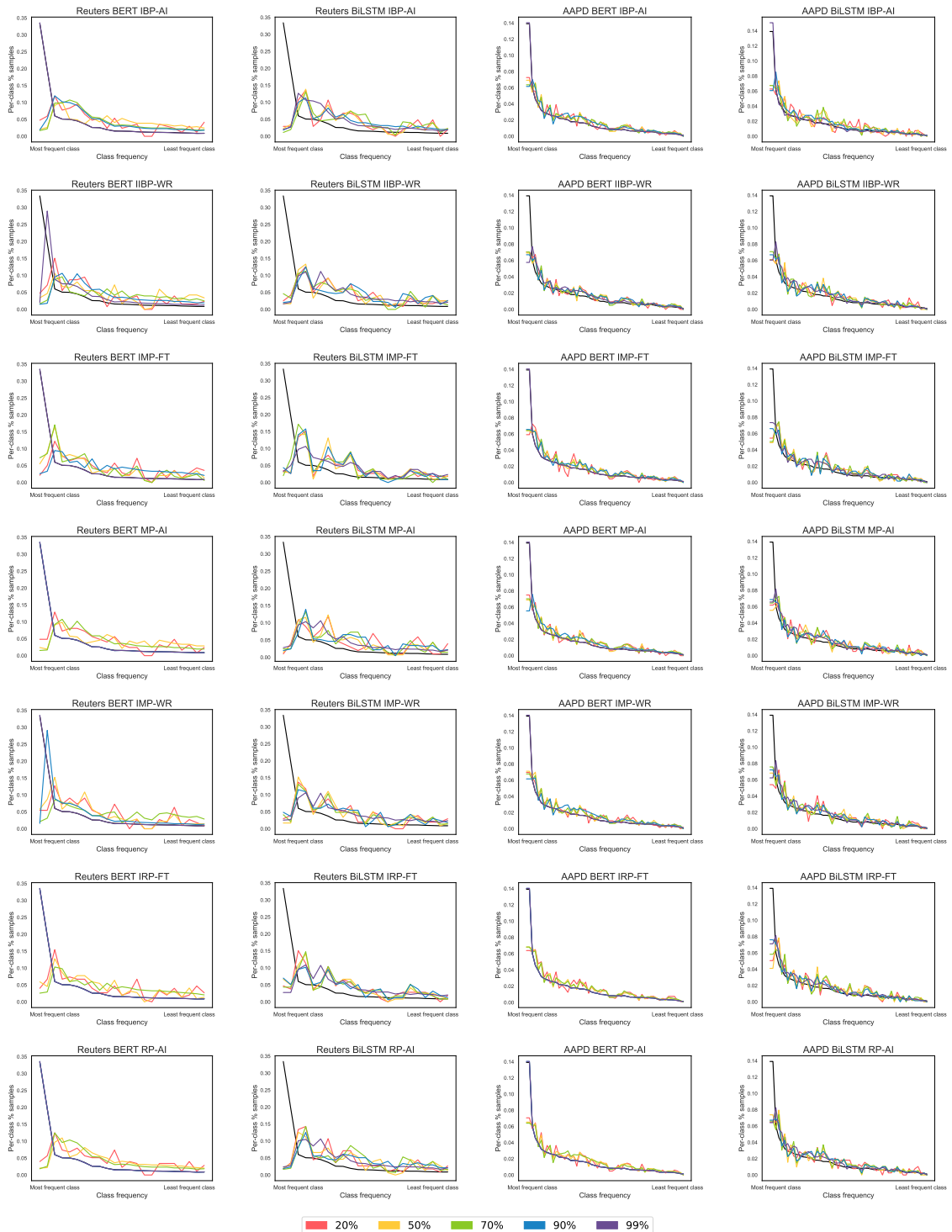


Figure 6: Distribution of all data points and of PIEs at 20% to 99% pruning, across classes sorted by frequency (x axis), for the multi-label datasets (test set).

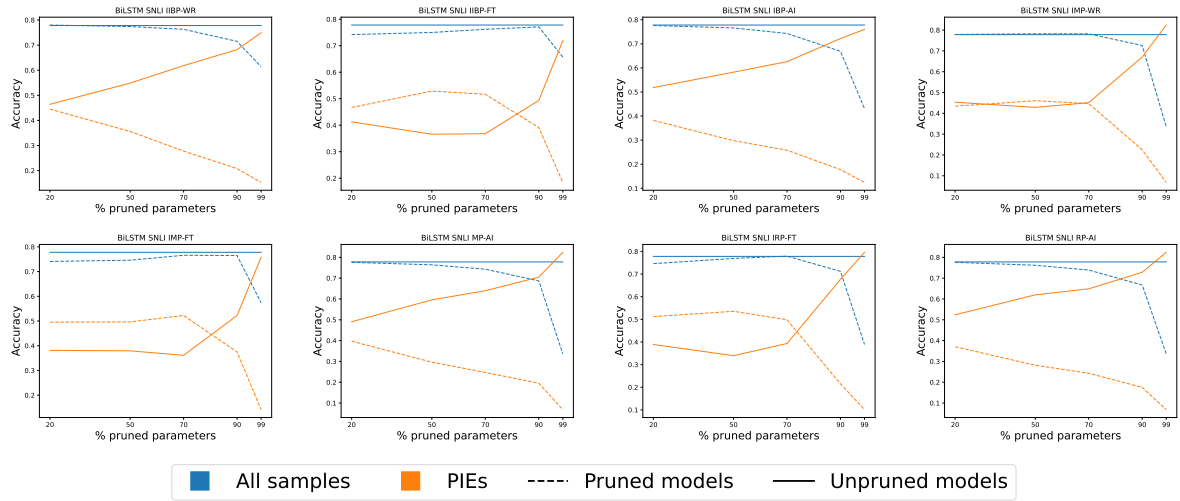


Figure 7: Accuracy of unpruned (black line) and pruned models on PIEs and all samples in the dataset per pruning method, across pruning thresholds (x-axis), over 30 initializations.

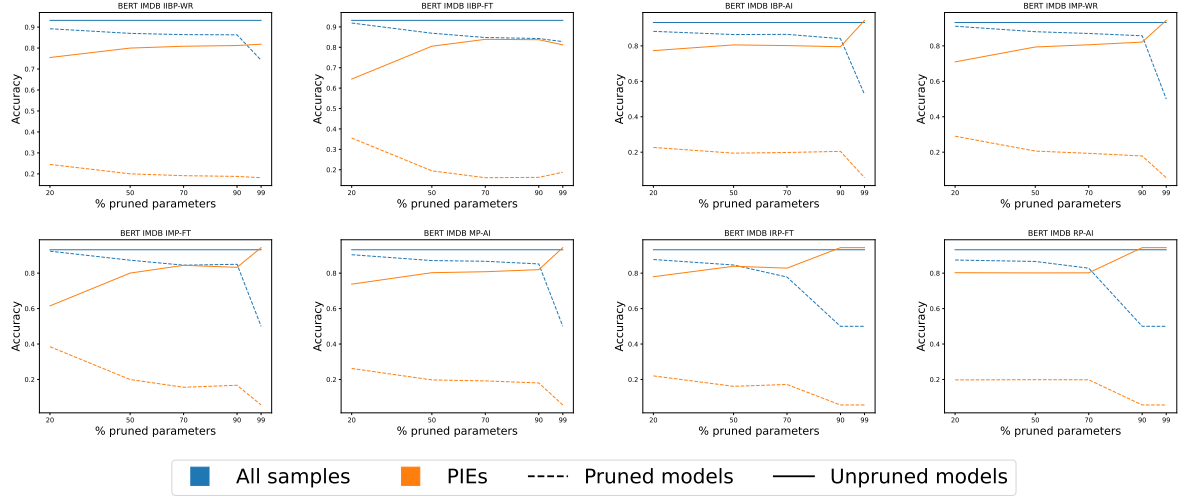


Figure 8: Accuracy of unpruned (black line) and pruned models on PIEs and all samples in the dataset per pruning method, across pruning thresholds (x-axis), over 30 initializations.

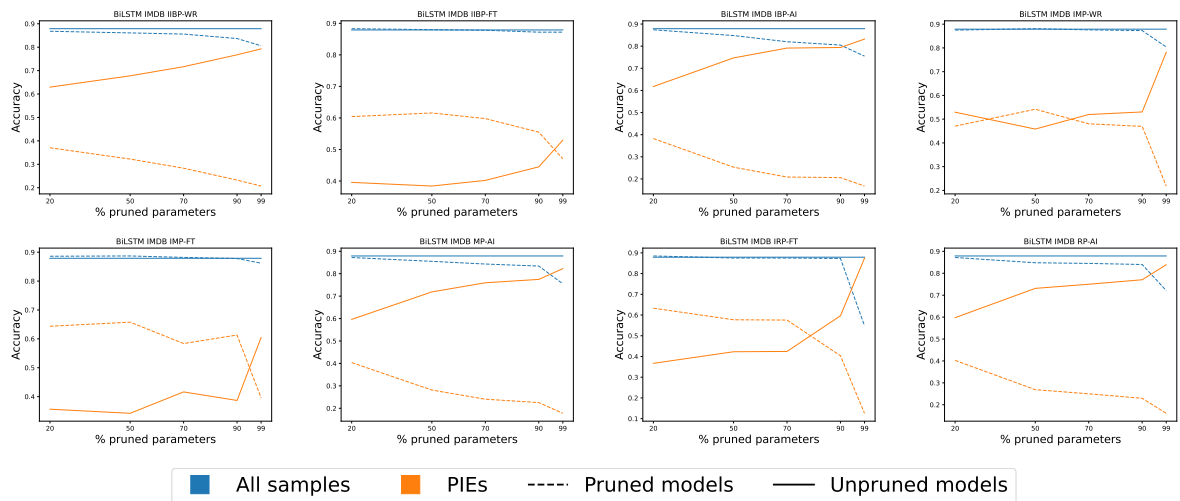


Figure 9: Accuracy of unpruned (black line) and pruned models on PIEs and all samples in the dataset per pruning method, across pruning thresholds (x-axis), over 30 initializations.

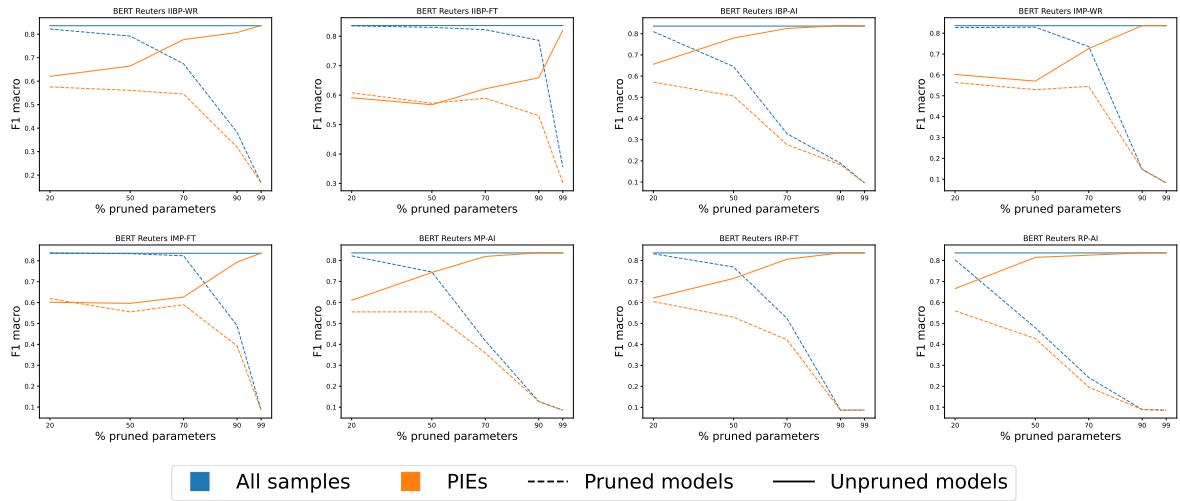


Figure 10: Accuracy of unpruned (black line) and pruned models on PIEs and all samples in the dataset per pruning method, across pruning thresholds (x-axis), over 30 initializations.

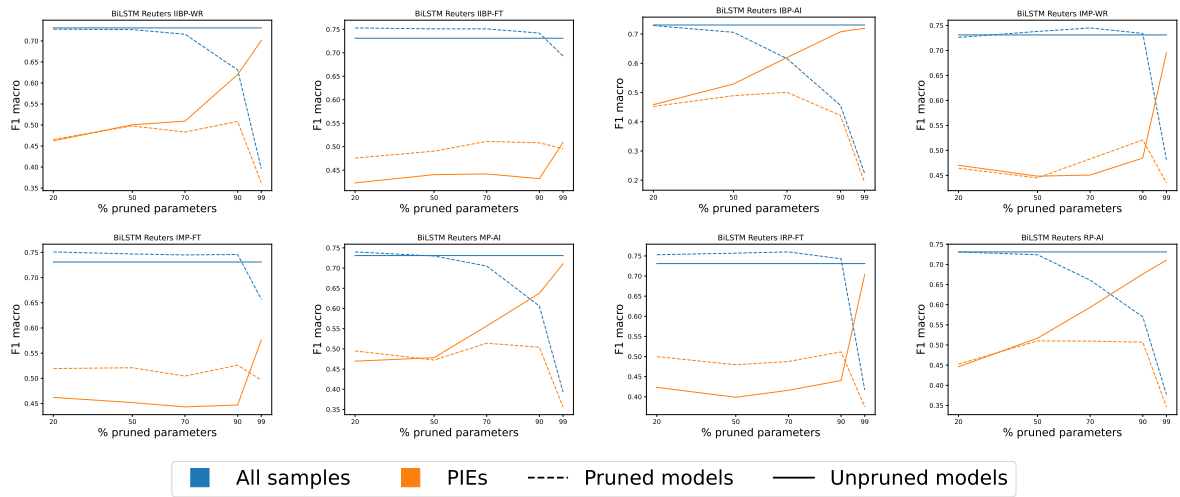


Figure 11: Accuracy of unpruned (black line) and pruned models on PIEs and all samples in the dataset per pruning method, across pruning thresholds (x-axis), over 30 initializations.

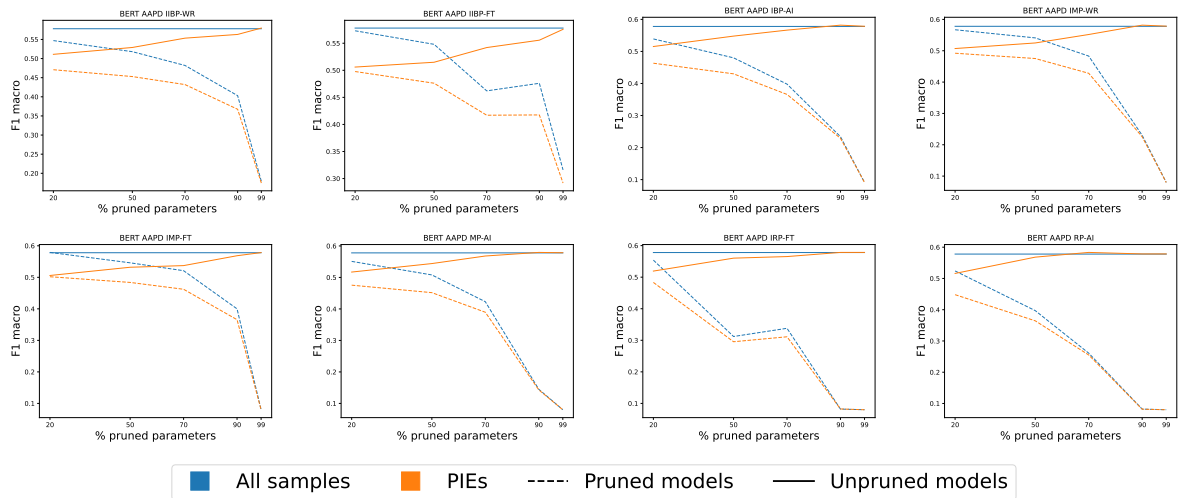


Figure 12: Accuracy of unpruned (black line) and pruned models on PIEs and all samples in the dataset per pruning method, across pruning thresholds (x-axis), over 30 initializations.

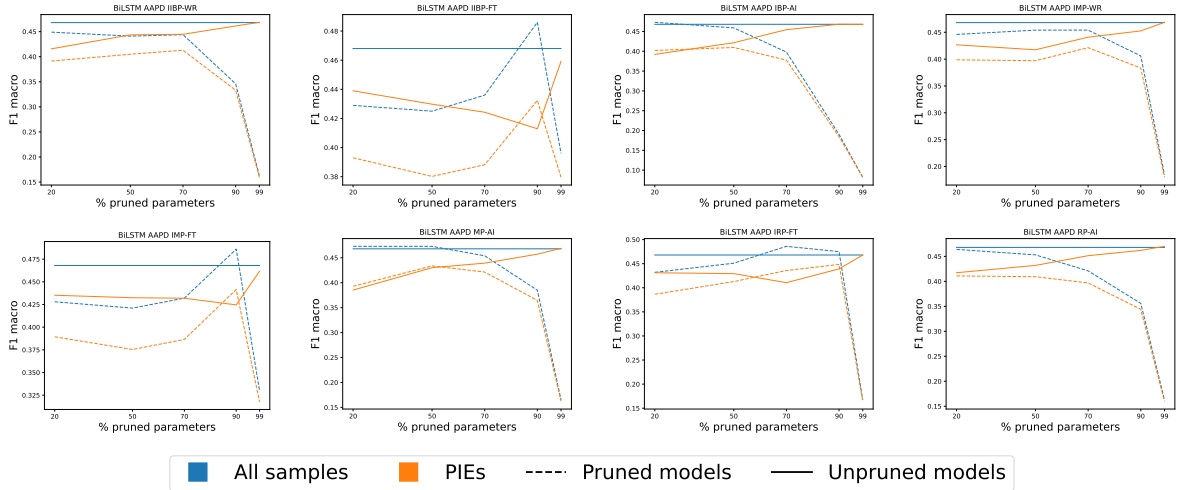


Figure 13: Accuracy of unpruned (black line) and pruned models on PIEs and all samples in the dataset per pruning method, across pruning thresholds (x-axis), over 30 initializations.

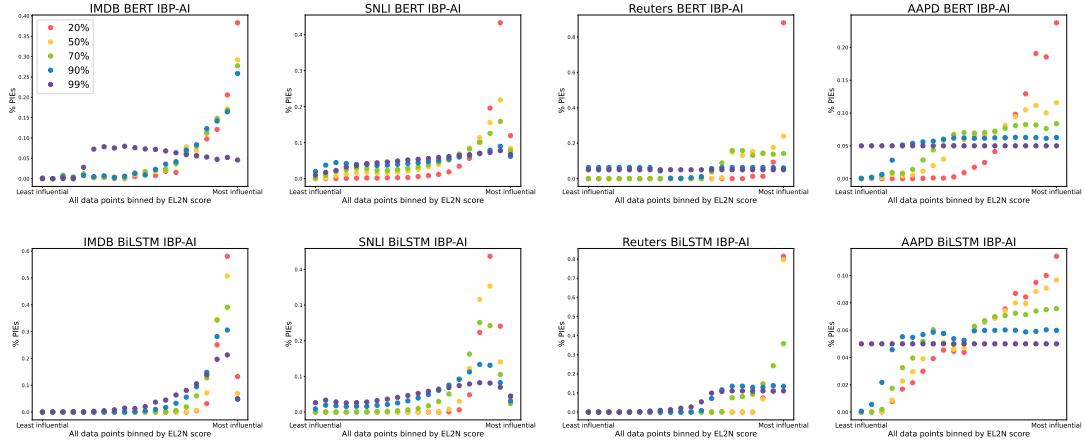


Figure 14: Percentage of data points that are PIEs (y axis) versus degree of influence (EL2N score) of all data points in the training set (x axis) for IBP-AI.

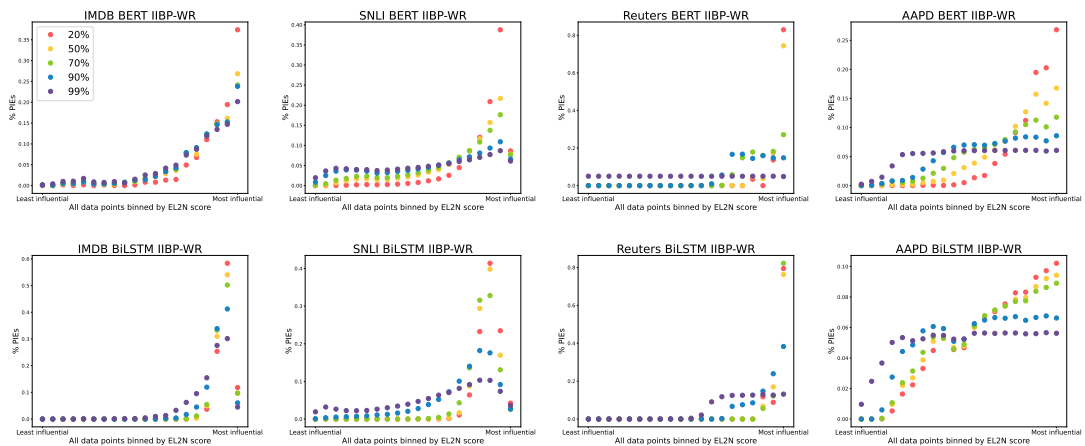


Figure 15: Percentage of data points that are PIEs (y axis) versus degree of influence (EL2N score) of all data points in the training set (x axis) for IIBP-WR at 20% and 99% pruning.

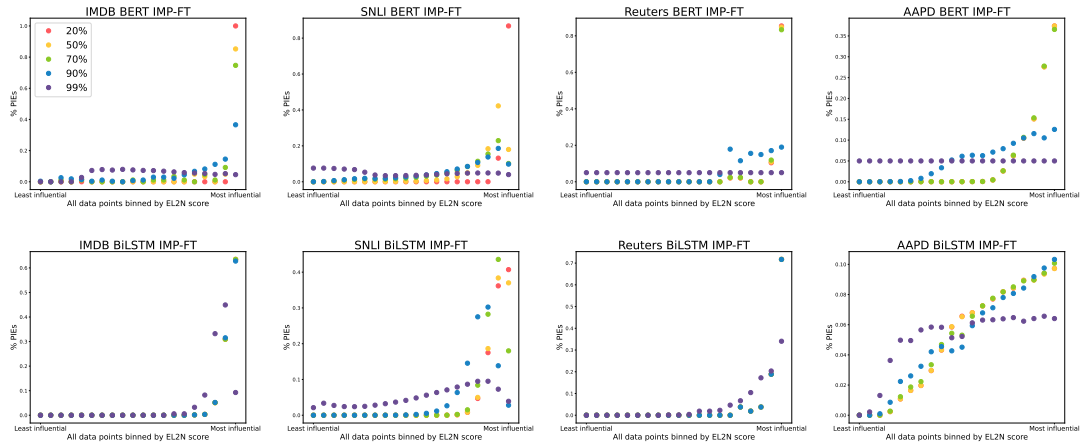


Figure 16: Percentage of data points that are PIEs (y axis) versus degree of influence (EL2N score) of all data points in the training set (x axis) for IMP-FT.

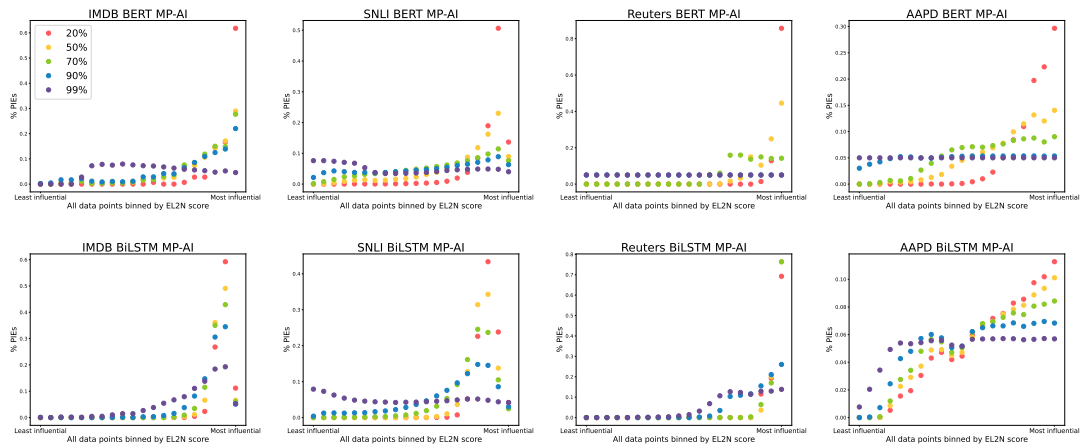


Figure 17: Percentage of data points that are PIEs (y axis) versus degree of influence (EL2N score) of all data points in the training set (x axis) for IMP-AI.

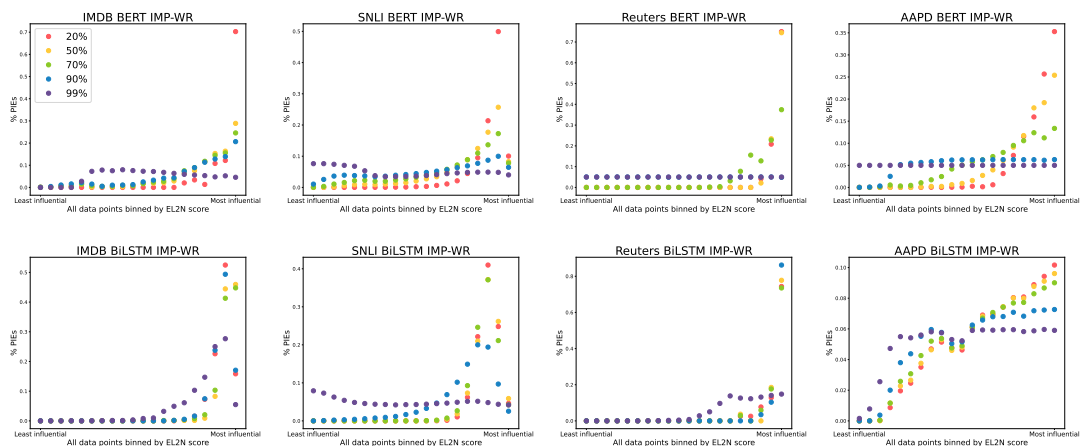


Figure 18: Percentage of data points that are PIEs (y axis) versus degree of influence (EL2N score) of all data points in the training set (x axis) for IMP-WR.

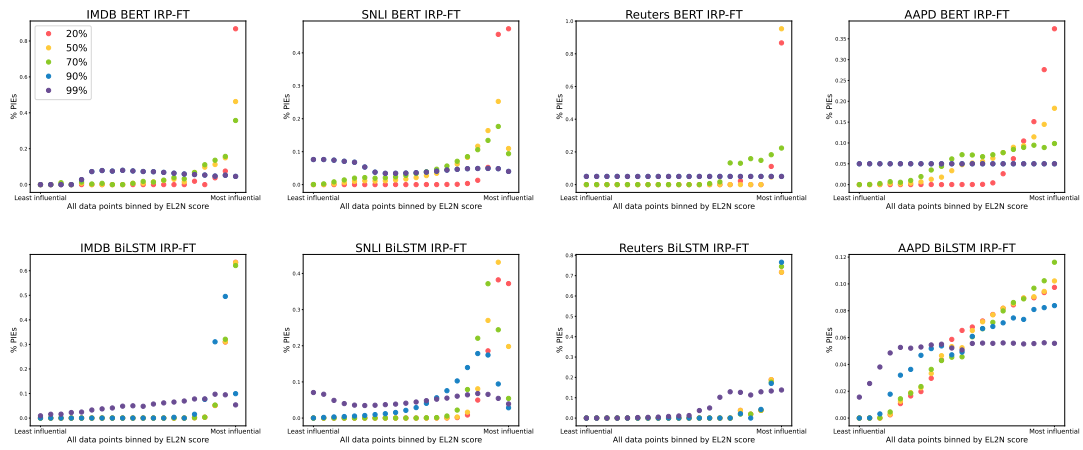


Figure 19: Percentage of data points that are PIEs (y axis) versus degree of influence (EL2N score) of all data points in the training set (x axis) for IRP-FT.

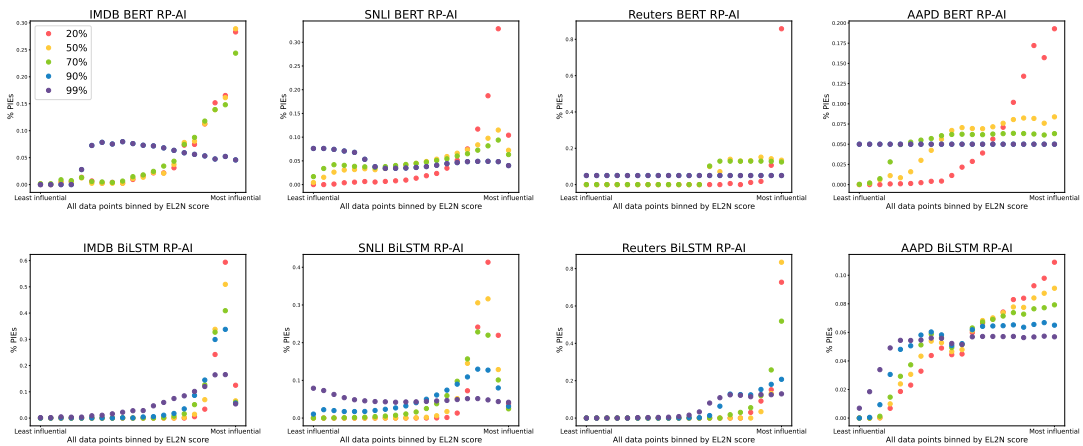


Figure 20: Percentage of data points that are PIEs (y axis) versus degree of influence (EL2N score) of all data points in the training set (x axis) for RP-AI.

1090 all our datasets. As shown in the remaining set-
 1091 tings, the more the disagreement between pruned
 1092 and unpruned model predictions, the harder it is to
 1093 observe a difference between the formal education
 1094 level needed to understand PIEs and the dataset.
 1095 Hence, on AAPD, we do not observe the same
 1096 behaviour obtained in the three remaining datasets.

1097 PIEs are overall longer than the text for all data
 1098 points. PIEs can have up to 1.13 and 1.9 more
 1099 tokens than the average number of tokens for a
 1100 sample in the dataset for IMDB, and Reuters re-
 1101 spectively. The behaviour can be observed with
 1102 both BERT and BiLSTM models. About the ratio
 1103 between the average number of tokens for the PIEs
 1104 and in all the samples of the dataset on SNLI and
 1105 AAPD datasets: we do not see the same behaviour
 1106 as in IMDB and Reuters. SNLI is mostly made
 1107 of short samples, hence it is harder to observe the
 1108 behaviour on such a dataset, even if the trend is
 1109 the same. On AAPD, the same observation on the
 1110 formal education level needed to understand holds
 1111 when discussing text length.

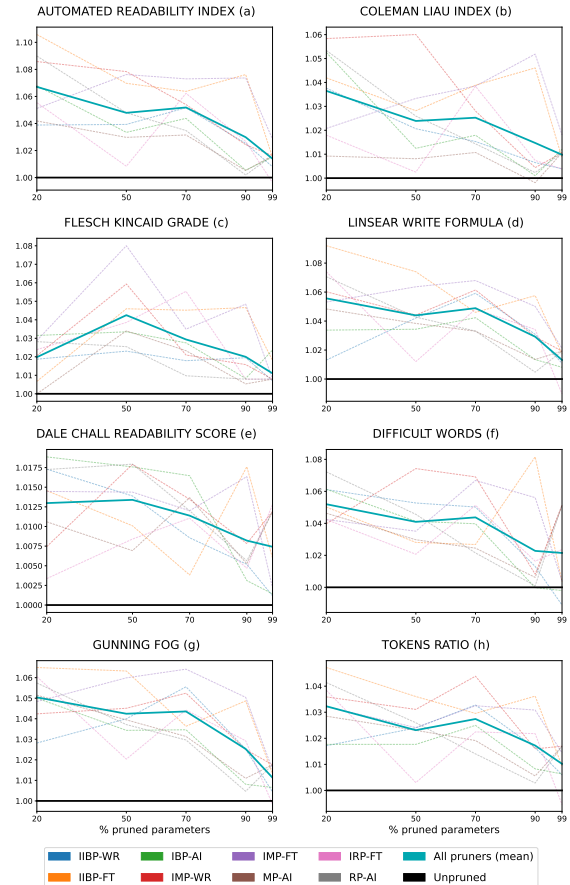


Figure 21: How the text of PIEs differs from the text of all data points, according to 7 readability scores (plots (a)-(g)) and text length (plot (h)). Ratio between the scores of PIEs and the scores of all data points (y axis), across pruning thresholds (x axis), for BiLSTM and SNLI. The solid black horizontal line represents equal scores in PIEs and all data points. The solid turquoise line is the mean score of all pruners. Any line above the solid black line means that PIEs are harder to understand (plots (a)-(g)) or have longer text (plot (h)), on average, than all data points.

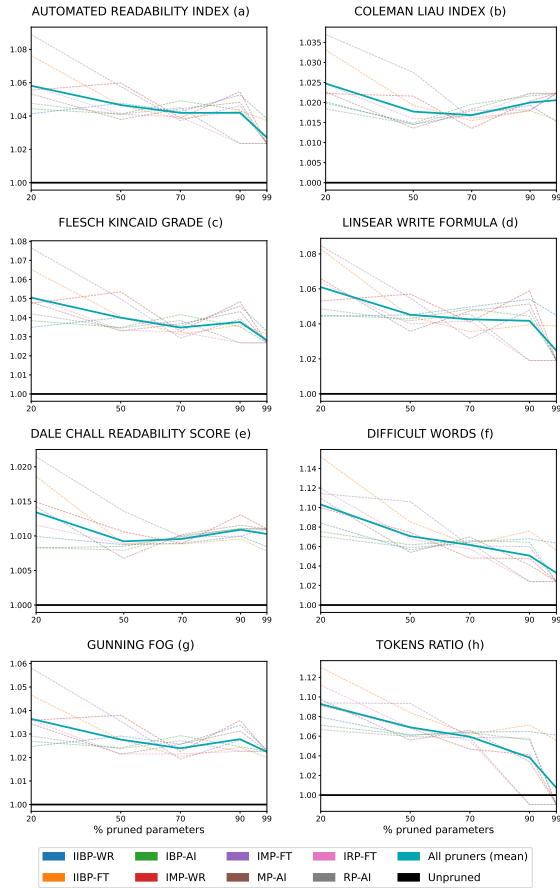


Figure 22: How the text of PIEs differs from the text of all data points, according to 7 readability scores (plots (a)-(g)) and text length (plot (h)). Ratio between the scores of PIEs and the scores of all data points (y axis), across pruning thresholds (x axis), for BERT and IMDB. The solid black horizontal line represents equal scores in PIEs and all data points. The solid turquoise line is the mean score of all pruners. Any line above the solid black line means that PIEs are harder to understand (plots (a)-(g)) or have longer text (plot (h)), on average, than all data points.

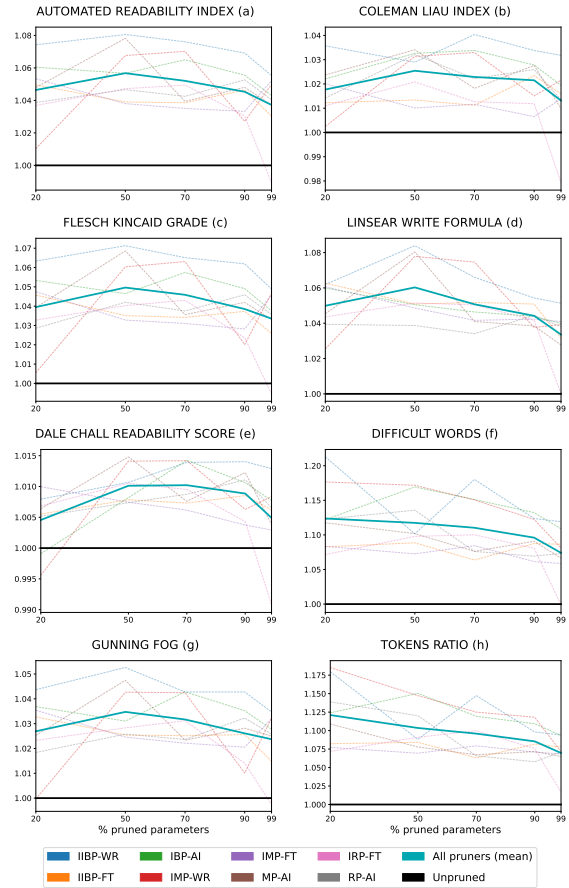


Figure 23: How the text of PIEs differs from the text of all data points, according to 7 readability scores (plots (a)-(g)) and text length (plot (h)). Ratio between the scores of PIEs and the scores of all data points (y axis), across pruning thresholds (x axis), for BiLSTM and IMDB. The solid black horizontal line represents equal scores in PIEs and all data points. The solid turquoise line is the mean score of all pruners. Any line above the solid black line means that PIEs are harder to understand (plots (a)-(g)) or have longer text (plot (h)), on average, than all data points.

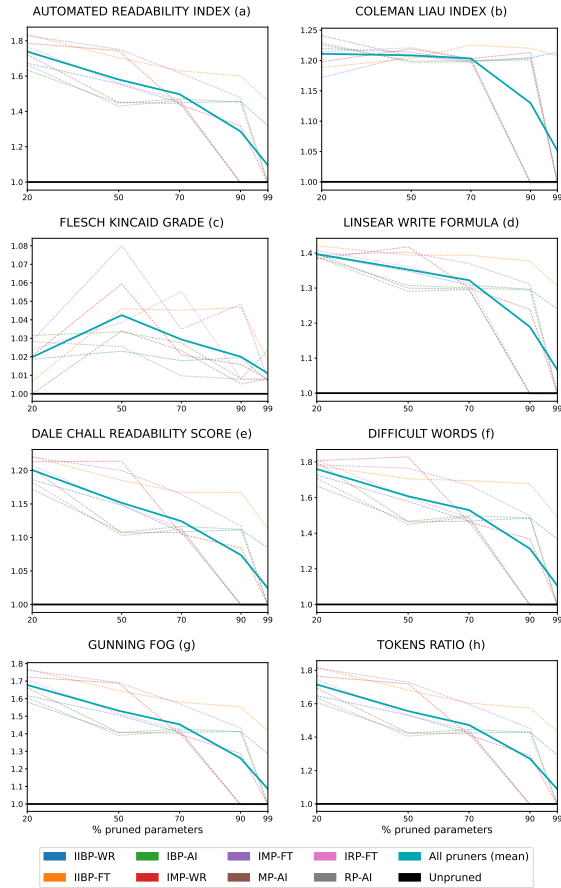


Figure 24: How the text of PIEs differs from the text of all data points, according to 7 readability scores (plots (a)-(g)) and text length (plot (h)). Ratio between the scores of PIEs and the scores of all data points (y axis), across pruning thresholds (x axis), for BERT and Reuters. The solid black horizontal line represents equal scores in PIEs and all data points. The solid turquoise line is the mean score of all pruners. Any line above the solid black line means that PIEs are harder to understand (plots (a)-(g)) or have longer text (plot (h)), on average, than all data points.

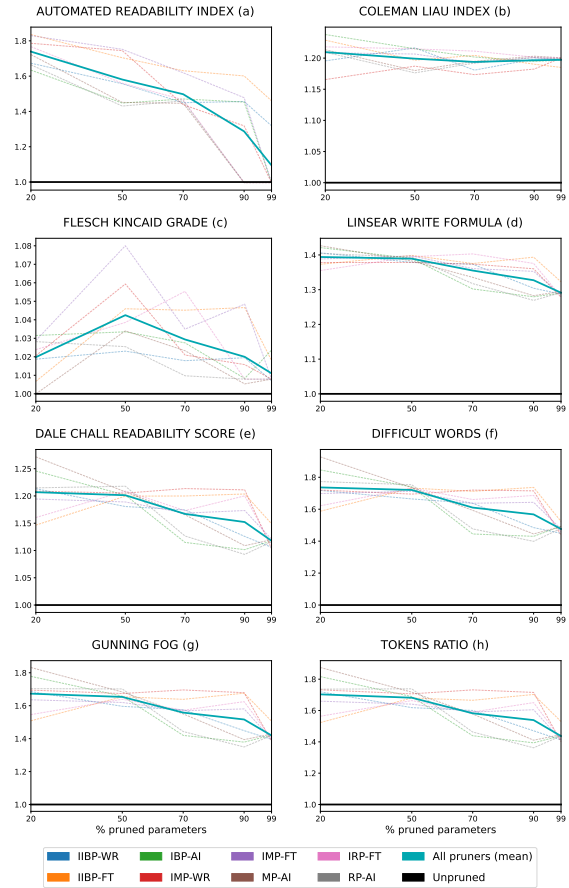


Figure 25: How the text of PIEs differs from the text of all data points, according to 7 readability scores (plots (a)-(g)) and text length (plot (h)). Ratio between the scores of PIEs and the scores of all data points (y axis), across pruning thresholds (x axis), for BiLSTM and Reuters. The solid black horizontal line represents equal scores in PIEs and all data points. The solid turquoise line is the mean score of all pruners. Any line above the solid black line means that PIEs are harder to understand (plots (a)-(g)) or have longer text (plot (h)), on average, than all data points.

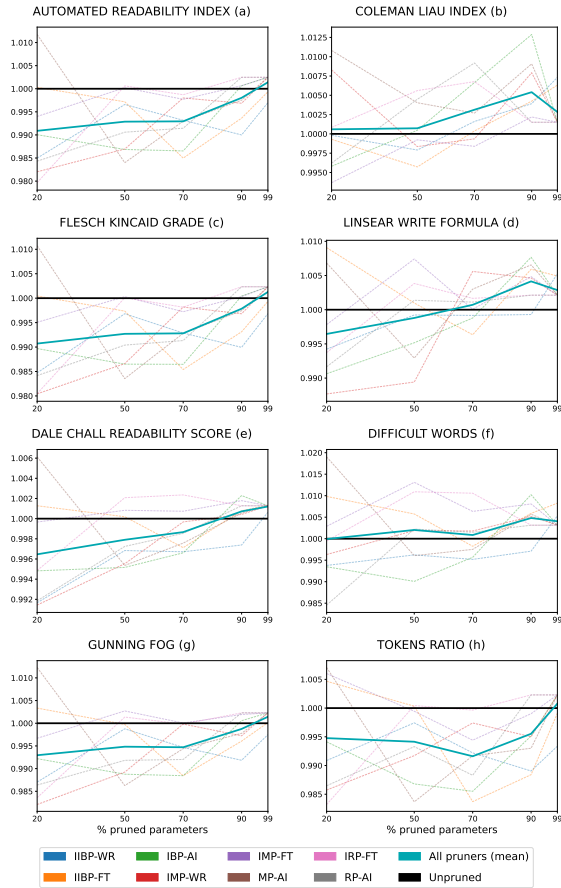


Figure 26: How the text of PIEs differs from the text of all data points, according to 7 readability scores (plots (a)-(g)) and text length (plot (h)). Ratio between the scores of PIEs and the scores of all data points (y axis), across pruning thresholds (x axis), for BERT and AAPD. The solid black horizontal line represents equal scores in PIEs and all data points. The solid turquoise line is the mean score of all pruners. Any line above the solid black line means that PIEs are harder to understand (plots (a)-(g)) or have longer text (plot (h)), on average, than all data points.

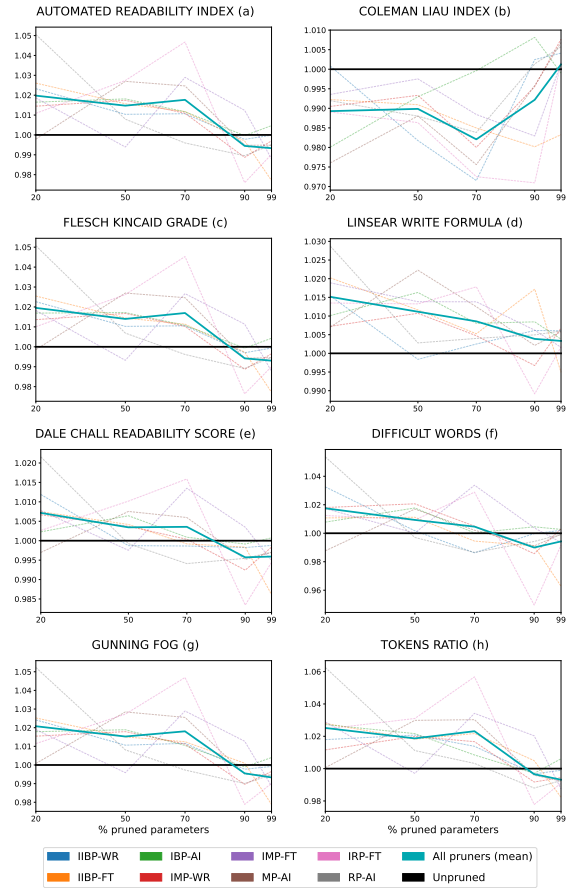


Figure 27: How the text of PIEs differs from the text of all data points, according to 7 readability scores (plots (a)-(g)) and text length (plot (h)). Ratio between the scores of PIEs and the scores of all data points (y axis), across pruning thresholds (x axis), for BiLSTM and AAPD. The solid black horizontal line represents equal scores in PIEs and all data points. The solid turquoise line is the mean score of all pruners. Any line above the solid black line means that PIEs are harder to understand (plots (a)-(g)) or have longer text (plot (h)), on average, than all data points.